Quark Propagation Through Cold QCD Matter

Important new information on the propagation of quarks through nuclear systems can be gained using CLAS with a 5.7 GeV electron beam. A systematic investigation over a range of nuclei is proposed, measuring hadronic multiplicity ratios, transverse momentum broadening, and, potentially, fragmentation functions. These measurements will provide significant new insight into the energy loss of quarks traversing the nuclear color field, and into the space-time characteristics of the hadronization process.

Experimental Collaborators:
Will Brooks, Kyungseon Joo, Jefferson Lab
Kim Egiyan, Yerevan Physics Institute
Ken Hicks, Ohio University
Franz Klein, Catholic University of America
Laird Kramer, Florida International University
Sebastian Kuhn, Lawrence Weinstein, Old Dominion University
Michael Vineyard, Union College
Kebin Wang, University of Virginia

Theoretical Collaborators:
Miklos Gyulassy, Columbia University
Boris Kopeliovich, Max-Planck-Institut fuer Kernphysik, Heidelberg
Larry McLerran, Brookhaven National Laboratory
Jan Nemchik, Institute of Experimental Physics SAV, Slovakia
Jianwei Qiu, Iowa State University
Ina Sarcevic, University of Arizona
Misak Sargsian, Florida International University
Mark Strikman, Pennsylvania State University
Xin-Nian Wang, Lawrence Berkeley National Laboratory

New collaborators are welcome

Table of Contents

Quark Propagation Through Cold QCD Matter

A proposal to Jefferson Lab PAC 22

The study of quark propagation through nuclear systems has never been more timely. This propitious situation results from the convergence of measurements in nuclei from Fermilab of the Drell-Yan process, from Hermes in deep inelastic scattering, and in the A-A and p-A programs at RHIC. Over the past decade there has been a rising level of theoretical interest and activity in nuclear processes at higher energy, in anticipation of the new data. An opportunity exists to make a definitive and unique set of measurements at Jefferson Lab, offering data of unprecedented statistical quality and kinematic breadth. Significant measurements can already be carried out with a 5.7 GeV beam; a follow-on measurement with an 11 GeV beam would provide broader kinematic coverage with an upgraded CLAS.

Executive Summary

The measurements proposed herein address two scientific thrusts of quark propagation through cold nuclei: hadronization and energy loss.

QUARK HADRONIZATION

Due to the property of confinement, a struck quark will evolve in space-time to produce multiple hadrons through the complex process of hadronization. This behavior is a unique distinctive of QCD. By studying the properties of leading particles emerging from deep inelastic scattering (DIS) on a range of nuclei, important information on the characteristic time-distance scales of hadronization can be determined as a function of several variables. At least two types of derived quantities will be employed in these studies. The first quantity is the hadronic multiplicity ratio, R_M^h , an observable that measures the ratio of numbers of hadrons emitted in light and heavy nuclei in DIS. A second class of studies will be to derive fragmentation functions from the data, to the extent possible. The quark fragmentation functions will be modified within the nuclear medium, and the A-dependence can be studied. Experimental tests of factorization at the boundary of the strong coupling regime of QCD, such as can be performed with this data, hold additional scientific interest.

QUARK ENERGY LOSS

As a struck quark traverses the color field presented by a nucleus, it scatters off the partons in the medium, losing energy primarily by radiation of gluons. This behavior, which is a fundamental prediction of quantum chromodynamics (QCD), may have a coherent character similar to that of the Landau-Pomeranchuk-Migdal effect in the QED energy loss of charged particles passing through atomic matter. This coherence, in combination with the non-Abelian nature of QCD radiation, predicts that the energy loss will be quadratic in the distance the quark travels through a nuclear medium, in strong contrast to the energy loss in quantum electrodynamics (QED). One observable exploited here which is sensitive to quark energy loss is the transverse momentum of leading hadrons produced in deep inelastic scattering. This transverse momentum (transverse to the virtual photon's direction) is expected to broaden measurably in heavy nuclei relative to light nuclei as a result of gluon radiation and multiple scattering, and hence provides a quantifiable measure of quark energy loss. It has also been predicted that one type of multiparton correlation function may be measured from this broadening. A second class of observables includes the fragmentation functions mentioned above, which are significantly modified by energy losses within the nuclear medium. Recent work has demonstrated that this quantity holds great promise for extracting partonic energy loss.

EXPERIMENTAL APPROACH

The number of leading positive pions in DIS events on four nuclear targets will be measured in CLAS and compared to existing CLAS data on deuterium and hydrogen, all with 5.7 GeV beam. These events will be characterized in ν, Q^2, z, and p_T with sufficient statistics to study two-dimensional distributions in pairs of these quantities. Lower-momentum correlated particles will be measured along with the leading positive pions, with reduced acceptance. In addition to leading positive pions, leading negative and neutral pions and protons will be measured to the extent permitted by particle identification. Exploratory measurements with charged kaons will also be carried out with lower statistics and limited kinematic coverage.

Introduction

Quantum Chromodynamics, the theory of the strong force, exhibits several exotic features that are totally different from the other known forces in the universe. One such feature is confinement, which may be described as the central puzzle of hadronic nuclear physics. Intimately related to confinement is the process of hadronization, where color flux tubes or strings acquire sufficient energy density to generate a spray of new objects that produce jets of particles in high energy collisions. A second facet of confinement is that colored objects such as isolated quarks or gluons may not be observed directly, so that their properties must be inferred through indirect means.

The subject matter of this proposal is the propagation of quarks through nuclear systems. The primary processes affecting quarks propagating through nuclei are (1) energy loss through gluon radiation and elastic partonic collisions, and (2) hadronization. In a typical high energy jet of a few hundred GeV, the relativistic boost given to the quark or gluon ensures that the entire process of hadronization takes place far from the point of interaction. However, at lower energies, there is a small window of opportunity where the hadronization distances are of the scale of nuclear diameters, while at the same time the kinematics can still isolate events where the initial state is a fast quark struck by a virtual photon (deep inelastic scattering). These processes are of great intrinsic interest: hadronization is intimately related to the non-Abelian character of QCD that leads to confinement, while gluon radiation is a direct manifestation of the QCD exchange boson. By studying these processes, one directly accesses the behavior of a (colored) quark propagating through a color field. In addition, a quantitative understanding of these phenomena is very important for understanding the data from RHIC, where propagation of quarks through the plasma involves the same phenomena but at elevated densities and temperatures (hence ‘cold’ QCD matter in distinction to ‘hot’).

Based on observations from recent experiments at Hermes[1], Jefferson Lab at 6 and 12 GeV will be an ideal place to study these colored objects as they traverse nuclear matter, and to characterize their energy loss and formation lengths of hadrons[2]. The advantages of Jefferson Lab and CLAS for these studies include:

- the right beam energy range such that much of the hadronization happens at nuclear distance scales
- sufficient luminosity to characterize hadronization as a function of multiple variables for multiple nuclei with good statistical accuracy, for any gas or solid target
- the capability of measuring correlated low-energy particles in coincidence with the leading ejectiles, both charged and neutral, up to high multiplicity

1. “Hadron Formation in Deep-Inelastic Positron Scattering in a Nuclear Environment,” A. Airapetian, et al., (Hermes Collaboration), Eur. Phys. J. C20 (2001) 479 and hep-ex/0012049, in which it is noted that for the 27 GeV energy of the positron beam, it appeared that most of the hadronization was already taking place outside the nucleus based on measurements on nitrogen. Subsequent experiments with lower beam energies and larger nuclei have since been performed in response, but the results have not yet been released.
2. See Letter of Intent LOI-01-108 for an overview of the combined 6 and 12 GeV program. Updates on the 12 GeV experiment are available from the Hall B web page.

CONTEXT

Employing CLAS for such measurements offers several unique advantages. One such advantage is large acceptance, which brings the ability to measure nearly all light charged particles emitted from the reaction (above 100-300 MeV/c) with high efficiency, in addition to measuring emitted neutral particles at a reduced efficiency. Thus, correlated soft particles associated with the leading hadrons can be studied, and radiative processes can be well characterized. This will provide information on the hadronization process, may potentially allow separation of coherent and incoherent diffractive processes, and may provide information related to the impact parameter. Secondly, the relatively high luminosity of 10^{34} $cm^{-2}s^{-1}$, in combination with the large acceptance, will afford high statistical accuracy over a wide range in kinematics, allowing multidimensional analysis of the above phenomena (e.g., in pairs of the variables ν or x, Q^2, z, and p_T) in unprecedented detail. The capability of being able to accommodate solid targets, cryogenic liquid targets, and even simultaneous multiple targets, allows great flexibility in the selection of the target sequence to study A dependencies. The initial measurement proposed here would be carried out with a 5.7 GeV beam, which will allow a first look at quark propagation at the lowest practical energies. The natural follow-on measurement would require the 11 GeV beam available with the upgrade of CEBAF and CLAS. This would bring a much wider range of kinematics accessible in a spectrometer with greater hermiticity, an order of magnitude increase in luminosity, and would fill the present gap in energy between the existing Hermes data and potential Jefferson Lab data at 6 GeV. A final noteworthy physics connection is to the RHIC program, where a quantitative understanding of quark propagation would greatly benefit the study of the quark-gluon plasma and its evolution in time. Acquiring a rich body of data such as is proposed here has a high probability of having an important impact on this field, as well as offering significant discovery potential for high-energy nuclear physics. The strong connections to the very recent Hermes and RHIC data, as well as recent Fermilab data, and the associated burst of theoretical work on these topics, underscore the timeliness of this topic.

Elementary Introduction to the Notation and Relevant Equations

In this section, a few familiar equations and concepts are presented in order to establish the notation for the rest of the proposal.

CROSS SECTIONS

The inclusive inelastic scattering cross section may be expressed for electrons of energy E' scattered into solid angle $d\Omega$ as:

$$\frac{d^3\sigma}{dE'd\Omega} = \left(\frac{d^2\sigma}{d\Omega}\right)_{Mott}\left[W_2(x,Q^2) + 2W_1(x,Q^2)\tan^2\frac{\theta}{2}\right] = \Gamma(\sigma_T + \varepsilon\sigma_L) = \Gamma\sigma_{tot} \quad \textbf{(EQ 1)}$$

where σ_{tot} is the total cross section for absorption of virtual photons, Γ is the flux of virtual photons, L and T denote the longitudinal and transverse components, ε is the virtual photon polarization, $x = \frac{Q^2}{2M\nu}$, and W_1 and W_2 are the structure functions.

At sufficiently high values of Q^2 and ν, the functions $F_1=2MW_1(x,Q^2)$ and $F_2=\nu W_2(x,Q^2)$ are nearly independent of Q^2, i.e., Bjorken scaling holds.

For semi-inclusive hadron production with one detected hadron, the differential cross section may be written as the product of the virtual photon flux factor times a hadron-production cross section:

$$\frac{d^6\sigma}{dE'd\Omega dp_h^3} = \Gamma\frac{d^3\sigma}{dp_h^3}(x, Q^2, z, p_T^2, \phi) \qquad \textbf{(EQ 2)}$$

where $z = \frac{E_{hadron}}{\nu}$, p_T is the component of the hadron momentum perpendicular to the direction of the virtual photon, and ϕ is the angle between the electron scattering plane and the hadron-virtual photon plane.

As an aside, the cross section that is differential in the hadron variables z, p_T, and ϕ can be decomposed into the familiar terms arising from various states of the photon polarization for unpolarized beam and target:

$$\frac{d^6\sigma}{dE'd\Omega dz dp_T d\phi} \sim [\sigma_T + \varepsilon\sigma_L + \varepsilon\sigma_{TT}\cos 2\phi + \sqrt{\varepsilon(\varepsilon+1)}\sigma_{TL}\cos\phi]$$

In this expression σ_T is the differential cross section for transverse unpolarized virtual photons, σ_L for longitudinal virtual photons, and σ_{TT} for transverse plane-polarized virtual photons, while the σ_{TL} term arises from longitudinal-transverse interference.

Using Equation 1 and Equation 2, an invariant structure function F may be defined that represents the hadron distributions per interacting electron:

$$F = \frac{E_h}{\sigma_{tot}}\frac{d^3\sigma}{dp_h^3}(x, Q^2, z, p_T^2, \phi) \qquad \textbf{(EQ 3)}$$

The *fragmentation function* D^h for a particular hadronic species *h* is defined in terms of the invariant structure function F as:

$$D^h(x, Q^2, z, p_T^2) = \pi\frac{\nu}{p_L}\langle F\rangle_\phi \qquad \textbf{(EQ 4)}$$

in which F has been averaged over ϕ; fragmentation functions can also be defined by averaging over other variables.

QUARK-PARTON MODEL

According to the quark-parton model, the function $F_2(x)$ is related to the quark distribution functions $q_i(x)$ in the target nucleon as

$$F_2 = x\sum_i e_i^2 q_i(x)$$

in which e_i is the quark charge, and the sum runs over all flavors of quark and antiquark. In the high Q^2 limit, F_1 is related to F_2 by the Callan-Gross relation $F_2=2xF_1$.

In this model it is assumed that a virtual photon is absorbed on a quark on a short time scale, and that the quark subsequently fragments on a much longer time scale. The fragmentation function is then expressed as

$$D^h(x, Q^2, z, p_T^2) = \sum_q \varepsilon_q(x, Q^2) D_q^h(x, Q^2, z, p_T)$$

in which ε_q is the probability that the fragmenting quark is of type q, and $D_q{}^h$ is a *quark fragmentation function*. This expression assumes that the fragments of the struck quark are kinematically separated from spectator quarks of the target. For electroproduction of hadrons, the probability function is given by the quark distribution functions introduced earlier as:

$$\varepsilon_q(x, Q^2) = e_q^2 q(x) / \sum_i e_i^2 q_i(x)$$

The *hadronic multiplicity ratio* R_M^h is defined by:

$$R_M^h(z, \nu) = \frac{\left\{\dfrac{N_h(z, \nu)}{N_e(\nu)}\right\}_A}{\left\{\dfrac{N_h(z, \nu)}{N_e(\nu)}\right\}_D} = \frac{\left\{\dfrac{\sum_f e_f^2 q_f(x) D_f^h(z)}{\sum_f e_f^2 q_f(x)}\right\}_A}{\left\{\dfrac{\sum_f e_f^2 q_f(x) D_f^h(z)}{\sum_f e_f^2 q_f(x)}\right\}_D} \qquad \textbf{(EQ 5)}$$

where the first ratio is the experimental ratio of hadrons to electrons in DIS events for nucleus A to deuterium (D), and the second ratio is the parton model expression for this quantity. This expression assumes the factorized form shown, where the fragmentation functions are independent of x. The factorization assumption can be tested experimentally.

As a final note, the expression *leading hadron* refers to the hadron in the event that has the largest momentum.

Quark Energy Loss: Scientific Significance and Present Status

Partonic energy loss through hot and cold QCD matter has been the subject of a number of studies since the mid-1980's, both experimental and theoretical. The theoretical status has recently been reviewed[3]. The basic mechanisms share a number of features in common with the electromagnetic energy loss of a charged particle in matter. The energy loss is both due to collisional losses and radiative losses; coherent phenomena may strongly influence the radiative processes, just as it does in QED.

INTRODUCTION

The two mechanisms thought to account for quark energy loss are collisional losses through partonic *multiple scattering,* and radiative losses through *gluon radiation* that are induced by the multiple scattering. These mechanisms are present in nuclear matter of any temperature, although the energy loss is much greater in hot, dense matter. The dominant mechanism, particularly for hot nuclear matter, is believed to be gluon radiation, which is predicted to have a novel quadratic energy loss behavior with distance under a particular set of conditions.

Energy loss of ordinary particles in ordinary matter is also characterized by radiation and multiple scattering. An important feature of this process is the Landau-Pomeranchuk-Migdal (LPM) effect[4] where destructive interference between bremsstrahlung radiation amplitudes induces a coherent effect. The destructive interference suppresses radiation relative to the Bethe-Heitler formula in kinematic regions where the radiation formation length is long compared to the mean free path. This effect (in QED) has recently been demonstrated experimentally[5]. Because the effect arises from general relativistic uncertainty principle arguments, it is expected that there would be an analogous effect in QCD. Early efforts to derive the non-Abelian analog of the LPM effect hinted that the effect was significant and that it was an important factor in deriving quark energy loss[6]. These studies also suggested the energy loss per unit length was also approximately constant, however other work at that time[7] that considered very large nuclei (large number of scatterings) indicated $\frac{-dE}{dx} \propto \sqrt{E}$.

3. "Energy Loss in Perturbative QCD," R. Baier, D Schiff, B.G. Zakharov, Annual Reviews of Nuclear and Particle Science, Volume 50 (2000), pg. 37.
4. L.D. Landau, I.Y. Pomeranchuk, Dokl. Akad. Nauk SSSR 92:535,735 (1953); A. B. Migdal, Phys. Rev. 103:1811(1956).
5. "Bremsstrahlung Suppression Due to the LPM and Dielectric Effects in a Variety of Materials," L. Anthony et al.[SLAC-E-146 Collaboration], Phys. Rev. D 56, 1373 (1997) and hep-ex/9703016.
6. "Multiple Collisions and Induced Gluon Bremsstrahlung in QCD," M. Gyulassy and X.-N. Wang, Nucl. Phys. B420, 583 (1994); "Landau-Pomeranchuk-Migdal Effect in QCD and Radiative Energy Loss in a Quark-Gluon Plasma," X.-N. Wang, M. Gyulassy, M. Plümer, Phys. Rev. D51, pg. 3436 (1995).
7. "Induced Gluon Radiation in a QCD Medium," R. Baier, Y.L. Dokshitzer, S. Peigné, D. Schiff, Phys. Lett. B 345 (1995) 277-286, and hep-ph/9411409.

Using a combination of data from the proposed experiment, its 12 GeV extension, and the HERMES data, it should be possible to study the transition from high to low ν, that is, the transition from quark propagation to hadron propagation in nuclei. The latter topic has recently been studied in quasifree kinematics[8].

RHIC CONNECTION

The dependence of quark energy loss on the medium density and temperature was proposed over a decade ago to be exploited as a signature of the formation of a hot, dense quark-gluon plasma in relativistic heavy ion collisions. A quantitative understanding of quark energy loss is essential to make definitive statements about the observations of jet quenching in relativistic heavy-ion collisions; there are numerous additional complications for a hot plasma that are not present for cold nuclei, such as thermal gluon absorption by propagating partons[9], and a highly non-equilibrated environment[10]. Fluctuations in the number of radiated gluons have been suggested to be very important for understanding the radiated energy loss of the highest energy jets, based on the first data from RHIC[11]. It has also been suggested that the cone of outgoing particles associated with a struck quark is much broader for hot, dense nuclear matter than for cold[12]. Although pA measurements are hoped to provide baseline understandings of the AA data at RHIC, these reactions are also not completely understood. A recent paper discussing the Cronin effect (the enhancement of high-p_T hadrons due to multiple interactions in nuclear matter) commented that there is not yet a quantitative explanation of this phenomenon, and as a result, using pA data to interpret AA data relies on parameters extracted with an incomplete understanding[13]. The effect of initial state interactions on partonic energy loss measurements has been studied for particular final state configurations[14]. A quantitative analysis of the RHIC data requires understanding such phenomena as initial state interactions, parton shadowing, and the Cronin effect in a complex thermodynamic environment. While new frameworks are being developed that are hoped to eventually accommodate the required level of complexity[15], these efforts are still at an early stage. It would clearly be beneficial to experimentally establish the energy loss characteristics systematically in simpler systems, as is proposed here.

In Figure 1 is shown a prediction for RHIC data of transverse momentum spectra for central collisions at RHIC for two different collision energies[16]. It gives some indication

8. "Quasifree (e,e'p) Reactions and Proton Propagation in Nuclei," D. Abbott et al., Phys. Rev. Lett. 80, 5072 (1998).
9. "Parton Energy Loss with Detailed Balance," E. Wang and X.-N. Wang, nucl-th/0106043.
10. "Radiative Energy Loss of High Energy Partons Traversing an Expanding QCD Plasma," R. Baier, Yu.L. Dokshitzer, A.H. Mueller, D. Schiff, Phys. Rev C58, pg. 1706 (1998)
11. "Jet Tomography of Au+Au Reactions Including Multi-Gluon Fluctuations," M. Gyulassy, P. Levai, and I. Vitev, nucl-th/0112071, 22 December 2001.
12. "Angular Dependence of the Radiative Gluon Spectrum and the Energy Loss of Hard Jets in QCD Media," R. Baier, Yu.L. Dokshitzer, A.H. Mueller, D. Schiff, Phys. Rev. C, Vol 60, 064902 (1999).
13. "Cronin Effect in Hadron Production Off Nuclei," B.Z. Kopeliovich, J. Nemchik, A. Schaefer, A.V. Tarasov, hep-ph/0201010, 3 Jan 2002.
14. "Medium-induced Parton Energy Loss in γ+Jet Events of High-Energy Heavy-Ion Collisions," X-N. Wang, Z. Huang, Phys. Rev. C 55, 3047 (1997); X.-N. Wang, Z. Huang, I. Sarcevic, Phys. Rev. Lett. 77, 231 (1996).

of the sensitivity of the calculations to the energy loss estimates. The difference between no energy loss and an energy loss of 0.5 GeV/fm at a given value of p_T tends to be more than one order of magnitude for few-GeV partons (at least in this calculation, which predates the RHIC data). It is clearly important to achieve a high degree of understanding of this quantity to extract the maximum information from these data.

COHERENT PHENOMENA

Understanding coherent aspects of QCD multiple scattering in detail is of intrinsic interest, and will also be important for understanding heavy ion collisions. A recent study using an expansion in opacity (essentially the mean number of collisions in the nuclear environment) inferred analytical expressions for totally coherent and totally incoherent limits of the gluon radiation cross section[17]. A second investigation focusing on the kinematic region where the LPM effect is not relevant (long gluon formation lengths relative to the nuclear size) showed that nuclear effects in that regime vanish for transverse momenta greater than 10 GeV in heavy ion collisions, and the largest medium enhancements of gluon bremsstrahlung took place in the range of 1-4 GeV. This underscores the relevance and importance of the measurements proposed here, which focus initially on the region of few-GeV quarks. Further, the degree of relevance of the LPM effect may provide measurable consequences, such as an energy loss that has both a linear term and a quadratic term in the distance travelled through the medium. It may be possible to sort out this dependence using a range of nuclei, from small to large. With the higher statistics available from the proposed experiment, one may also be able to search for evidence of the Cronin effect at $p_T > 1$GeV.

15. E.g., “Jet Energy Loss in Hot and Dense Matter,” I. Vitev, M. Gyulassy, P. Levai, nucl-th/0204019, 5 Apr 2002; “Reaction Operator Approach to Multiple Elastic Scatterings,” M. Gyulassy, P. Levai, I. Vitev, nucl-th/0201078, 29 Jan 2002; “Reaction Operator Approach to Non-Abelian Energy Loss,” M. Gyulassy, P. Levai, I. Vitev, Nucl. Phys. B594 (2001) 371 and nucl-th/0006010; “Non-Abelian Energy Loss at Finite Opacity,” M. Gyulassy, P. Levai, I. Vitev, Phys. Rev. Lett. 85, (2000) 5535.
16. “Jet Quenching and Azimuthal Anisotropy of Large p_t Spectra in Noncentral High-Energy Heavy-Ion Collisions,” X.-N. Wang, Phys. Rev. C, 63, 054902 (2001).
17. “Gluon Radiation Off Hard Quarks in a Nuclear Environment: Opacity Expansion,” U.A. Wiedemann, Nucl. Phys B588(2000) 303 and hep-ph/0005129; see also “Transverse Dynamics of Hard Partons in Nuclear Media and the QCD Dipole,” U.A. Wiedemann, Nucl. Phys. B582 (2000) 409 and hep-ph/0003021.

FIGURE 1. Predicted distributions of transverse momenta in relativistic heavy ion collisions.

PHYSICAL REVIEW C 63 054902

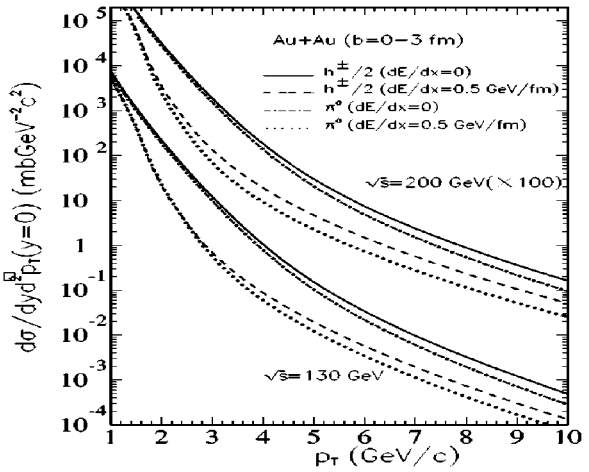

Transverse momentum spectra of charged hadrons (solid) and π^0 (dot-dashed) in central Au+Au collisions at $\sqrt{s}$ = 200 and 130 GeV without energy loss and with $dE/dx = 0.5$ GeV/fm (dashed lines for charged hadrons and dotted lines for π^0).

MODIFIED FRAGMENTATION FUNCTIONS

Recent studies of partonic energy loss via deep inelastic scattering (DIS) off nuclei[18 19] showed that it is possible to quantify the effects of multiple scattering and gluon radiation via a medium modification of the quark fragmentation functions in pQCD. This treatment considers the parton as off-shell, unlike several earlier treatments; in addition, finite-size nuclei are considered. The effective fragmentation functions and the modified DGLAP evolution equations were derived using the generalized factorization of twist-four parton distributions in hard processes. The resulting functions depend on both the diagonal and off-diagonal twist-four parton distributions in nuclei. The LPM interference pattern is clearly evident in their theoretical results. The validity of the generalized factorization up to twist-four has been proven for hard processes involving both hadrons and nuclei[20]. The most recent results from this work[21] (shown in Figure 2 and Figure 3) appear to demonstrate the novel quadratic behavior of the gluon-radiation portion of the energy loss. If this result is substantiated by further studies, it would constitute a stunning validation of the ideas developed over the past 15 years by a broad contingent of

18. "Multiple Scattering, Parton Energy Loss, and Modified Fragmentation Functions in Deeply Inelastic eA Scattering," X. Guo, X.-N. Wang, Phys. Rev. Lett. 85, pg. 3591 (2000); "Multiple Parton Scattering in Nuclei: Parton Energy Loss," X.-N. Wang, X. Guo, hep-ph/0102230, 19 Feb 2001. See also "Energy Loss of Hard Partons in Nuclear Matter," U.A. Wiedemann, Nucl. Phys. A 690(2001) 731 and hep-ph/0103332.

19. "Multiple Parton Scattering in Nuclei: Twist-Four Nuclear Matrix Elements and Off-Forward Parton Distributions," J. Osborne, X.-N. Wang, hep-ph/0204046, 4 April 2002.

20. J. W. Qiu, G. Sterman, Nucl. Phys. B 353, 105 (1991); J.W. Qiu, G. Sterman, Nucl. Phys. B 353, 137 (1991).

researchers. In this paper, a one-parameter formulation of the energy loss behavior is fixed by fitting to the krypton data from Hermes DIS, then predicting the behavior for nitrogen.

Predictions from the Wang model [18], [21] for the energy loss in the data that can be measured in CLAS with 5.7 GeV are shown in Figure 4. The present version of the model requires ν be significantly greater than the proton mass, and Bjorken x not too large, therefore the point chosen for the calculation is for $\nu = 5$ GeV, $Q^2 = 2$ GeV^2 which will be accessible with good statistics for the data from this proposal (as can be seen later in Figure 15 in the section on expected results). This calculation neglects the hadronization process, predicting only the effect of quark energy loss. An interesting feature of the prediction in Figure 4 is the 'anti-absorption' seen at small z. This is presumably due to the redistribution of the events, shifting events at high z to lower z. Another noteworthy feature is the predicted absorption difference at $z = 0.7$, which indicates a much larger gap between the gold and krypton targets than between the argon and krypton targets. This is very different from the prediction of the gluon bremsstrahlung model shown in Figure 15; in addition, the slopes of the curves at $z = 0.5$ are quite different. The proposed data will be able to easily distinguish between the predictions of these two models.

21. "Jet Tomography of Dense and Nuclear Matter,'' hep-ph/0202105, E. Wang and X.N. Wang, February 2002; "Multiple Scattering, Parton Energy Loss, and Modified Fragmentation Functions in Deeply Inelastic eA Scattering," X. Guo, X.-N. Wang, Phys. Rev. Lett. 85, 3591(2000).

FIGURE 2. Predicted nuclear modification of jet fragmentation function compared to HERMES data, as a function of z.

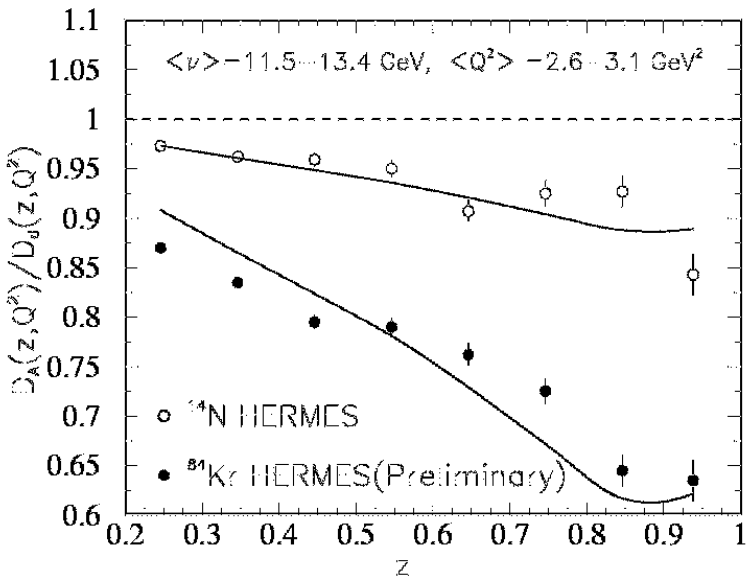

Predicted nuclear modification of jet fragmentation function is compared to the HERMES data [10] on ratios of hadron distributions between A and D targets in DIS.

Further study is required to determine in which kinematic regions CLAS can separate current fragmentation (particles produced by hadronization of the struck quark) from target fragmentation (particles produced from the residual nucleon). Additional absorption and redirection of target fragments may improve the ability to separate these processes for the heavier nuclei. Some experimental information exists on the extent of heating of the residual nucleus[22]; those data indicate relatively little heating except for the heaviest nucleus in that experiment (^{208}Pb). This may indicate the knocked-out particle fragments have little interaction with the residual system[23], however, these measurements were performed with much higher beam energy. At the least it will be possible to measure the nuclear dependence of ratios of hadron multiplicity R_M^h , to tag low-energy correlated particles, and to study the properties of leading hadrons as a function of several intrinsic variables. In any case it is clear that particles with large z, e.g. z > 0.5, have resulted from a current fragmentation process. The prospects for extension to smaller z will require further study of the experimental data.

22. "Nuclear Decay Following Deep Inelastic Scattering of 470 GeV Muons," M.R. Adams, . . ., K.H. Hicks, et al. (E665 Collaboration), Phys. Rev. Lett. 74, 5198 (1995); Erratum-ibid. 80, 2020(1998).

23. "Soft Neutron Production in DIS: a Window to the Final State Interactions," M. Strikman, M. G. Tverskoii, M. B. Zhalov, Phys. Lett. B 459, 37(1999), nucl-th/9806099.

FIGURE 3. Predicted nuclear modification of jet fragmentation function compared to HERMES data, as a function of ν.

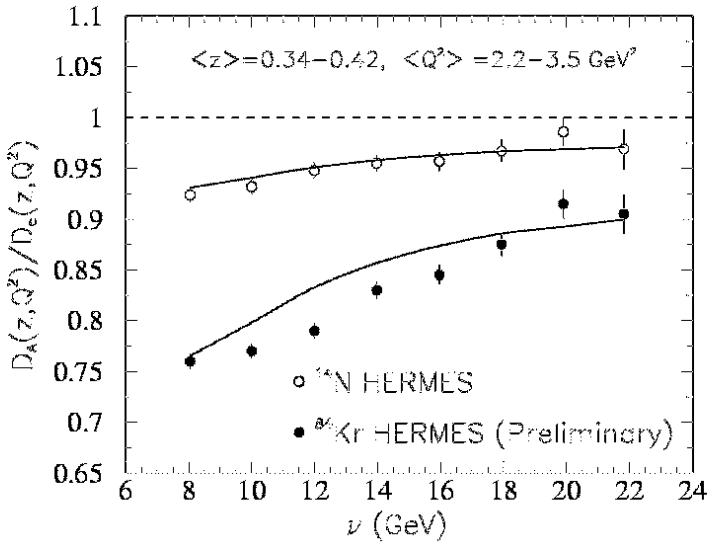

Energy dependence of the nuclear modification compared with the HERMES data [10].

It should also be noted that the study of jet physics at the high-energy end of the spectrum continues to be an actively developing field. Refinements in reconstruction and analysis of high energy jets continue to bring new insights from theory and phenomenology, which could have relevance to the low-energy regime. A recent discussion has compared several different thrusts of jet physics; one conclusion was that approaches including multiple parton scattering appear to give a better description of the data (such as implemented in PYTHIA), implying that secondary processes introducing multiparton correlations have a more important role than previously believed[24].

24."Summary: Working Group on QCD and Strong Interactions," E. Berger, S. Magill, I. Sarcevic, et al., hep-ph/0201146, February 2002.

FIGURE 4. Predicted behavior from the Wang model for the z dependence of the hadronic multiplicity ratio for the data from this proposal for ν = 5 GeV and Q^2=2 GeV^2. Note the 'anti-absorption' predicted for small z. See text for more discussion. These predictions are quite different from the gluon bremsstrahlung model, see Figure 15b.

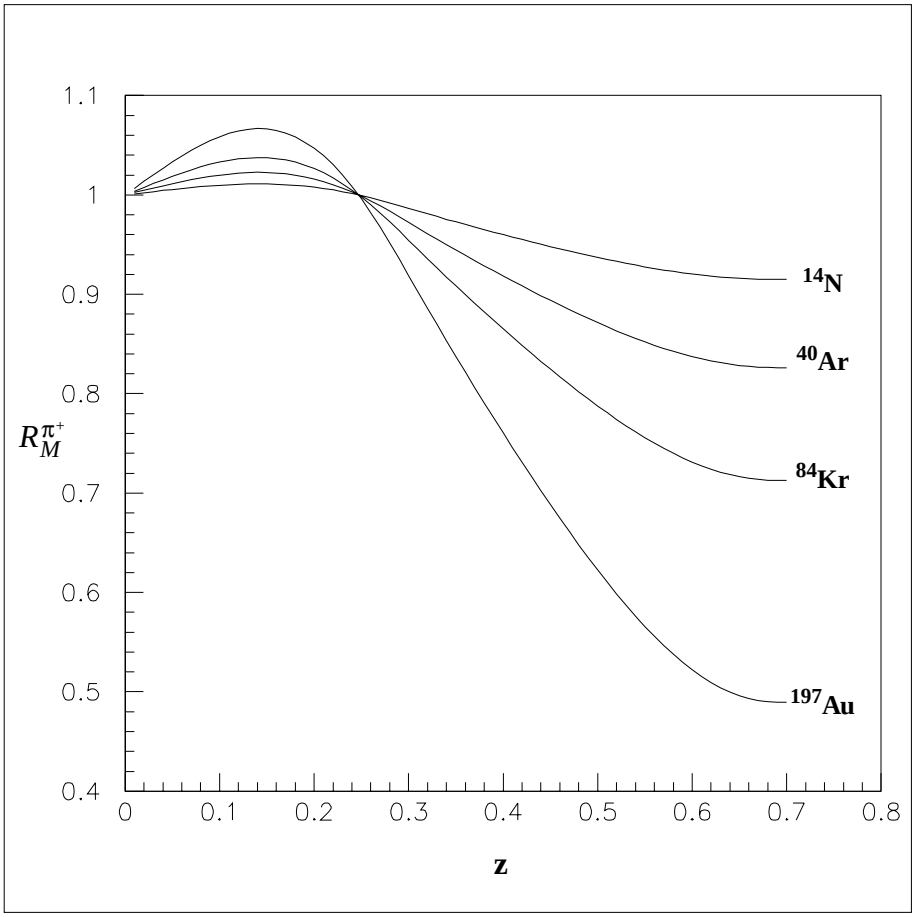

TRANSVERSE MOMENTUM BROADENING

With the same parameter, the above authors can compare to the nuclear broadening of the transverse momentum of the Drell-Yan dilepton production in pA collisions and find it to be consistent with the experimentally quoted value[25] of:

$$\Delta\langle p_T^2\rangle \equiv \langle p_T^2\rangle_A - \langle p_T^2\rangle_D \approx 0.021A^{1/3}\ \text{GeV}. \qquad \textbf{(EQ 6)}$$

25. "High-Energy Hadron-Induced Dilepton Production from Nucleons and Nuclei," P.L. McGaughey, J.M. Moss, and J.C. Peng, Ann. Rev. Nucl. Part. Sci. 49 (1999) 217-253, and hep-ph/9905409.

Observation of this transverse momentum broadening for larger nuclei relative to small nuclei is a direct indication of multiple scattering within the nuclear medium. At least two pieces of information can be obtained from the experimental measurement of this quantity. First, it is possible to derive[26] a simple formula from pQCD that yields the partonic energy loss directly from the momentum broadening shown in Equation 6:

$$dE/dx \approx \frac{\alpha_s}{\pi} N_c \langle k_\perp^2 \rangle_L \qquad \textbf{(EQ 7)}$$

where N_c is the number of colors and the average is taken over a system of length L. Under plausible assumptions, this leads to a quadratic dependence of the total energy loss on the path length. Interestingly, deviations from this quadratic dependence have been noted in recent studies using the opacity expansion[27]. These deviations occur at small path lengths, which are relevant for this proposal; they arise from destructive interference between hard and medium-induced radiation.

A second topic that may be addressed with momentum broadening is multiparton correlations[28]. Of the many multiparton correlation functions in QCD, one connects very directly with transverse momentum broadening. This is the function that represents the correlations between hard quarks and soft gluons. An important contribution of the data from this proposal would be to test and refine the multiple-scattering theory that is necessary to describe high-energy nuclear interactions.

PREVIOUS ESTIMATES

Theoretical estimates for the numerical value of the partonic energy loss have varied over a wide range over the past decade. Some of the variation is due to the 'learning curve' of understanding how to properly extract this information from experimental data, which can present subtle problems for some reactions, such as the role played by nuclear shadowing. Energy loss estimates for cold nuclei include: 1 GeV/fm from the gluon distribution of the nucleon, and 2 GeV/fm from studies of dijets (both for 10 fm nuclear thickness)[26]; 2.73 GeV/fm from a sophisticated analysis of Drell-Yan lepton pair production in several nuclei (2.32 GeV/fm from an earlier analysis of the same data, ~0. GeV in even earlier analyses)[29]; and 0.5 GeV/fm for a 10 GeV quark in a gold nucleus, assuming a Gaussian nuclear distribution of the form:

---

26. "Radiative Energy Loss and $p_\perp$ Broadening of High Energy Partons in Nuclei,", R. Baier, Yu. L. Dokshitzer, A. H. Mueller, S. Peigne, and D. Schiff, Nucl. Phys. B484, 265 (1997) and hep-ph/9608322; "Energy Loss and $p_\perp$ Broadening of High Energy Partons in Hot and Cold QCD Matter," A. Mueller, Nuclear Physics A610 pg. 459c (1996).

27. "Energy Loss of Hard Partons in Nuclear Matter," U.A. Wiedemann, Nucl. Phys. A690 (2001) 731 and hep-ph/0103332.

28. "Probing Quark-Gluon Correlation Functions," X. Guo, J.-W. Qiu, Phys. Rev. D 61, 096003 (2000); M. Luo, J.-W. Qiu, G. Sterman, Phys. Lett. B 279, 377 (1992); "Anomalous Nuclear Enhancement in Deeply Inelastic Scattering and Photoproduction," M. Luo, J.-W. Qiu, G. Sterman, Phys. Rev. D 50, 1951 (1994).

29. "Energy Loss versus Shadowing in the Drell-Yan Reaction on Nuclei," M. B. Johnson, B.Z. Kopeliovich, I.K. Potashnikova, P. L. McGaughey, J. M. Moss, J. C. Peng, G. Garvey, M. Leitch, C. N. Brown, D.M. Kaplan, hep-ph/0105195, 18 May 2001;"Energy Loss of Fast Quarks in Nuclei," M.B. Johnson, B.Z. Kopeliovich, I.K. Potashnikova, and the FNAL E772 Collaboration, Phys.Rev.Lett. 86 (2001) 4483-4487, and hep-ex/0010051. These authors identify several distinct classes of energy loss contributions for this reaction.

$$\rho(r) \sim \exp\left(\frac{-r^2}{2R_A^2}\right), \quad R_A = 6.5 \quad fm$$

in the very recent analysis of Hermes data from [21], which is equivalent to ~1 GeV/fm over a distance of 10 fm.

FACTORIZATION

Most of these studies rely in some measure on perturbative QCD (pQCD) and factorization between hard and soft physics. The measurements proposed here span a region of kinematics. In the lower-energy portion of this range, it is likely that these assumptions will not be valid, unless some quantitative version of quark-hadron duality can be invoked. In the higher-energy range, perturbative ideas and factorization may be applicable. The calculations mentioned in [18] appear to describe the Hermes data in a range of Q^2 from 2.6-3.1 GeV^2. These authors have studied the applicability of factorization of fragmentation functions at these low momentum transfers. A recent paper has investigated the connection between twist-four nuclear matrix elements and generalized parton distributions, testing the accuracy of factorization assumptions made for very large nuclei[19]. They find that the factorization is reasonably good for regions where the momentum fraction carried by the gluon field is not large. Their results are limited to a kinematic region in which ordinary parton distributions can replace the generalized parton distributions which would normally be required[30], and they make specific tests for $Q^2 = 2.5$ GeV^2 and $Q^2 = 5.0$ GeV^2. These authors also suggest that generalized parton distributions could be probed in multiple parton scattering processes in a nucleus, which, if substantiated, would offer interesting possibilities to connections to other HERMES and Jefferson Lab experiments. Another recent study examined the extension of the factorization formalism of pQCD to the soft rescattering associated with hard processes in nuclei[31], summarizing a series of investigations over the past decade[32]. They conclude that the nuclear effects caused by multiple scattering can be consistently calculated in pQCD using generalized factorization theorems, and that twist-4 terms can provide new insights into nonperturbative QCD.

The applicability of perturbative calculations down to parton energies of 3 - 4 GeV is not theoretically known in general. Some theoretical tests include checking the size of higher-order terms in α_s, and varying the renormalization, factorization, and fragmentation scales to check the sensitivity of the results. The observation of early onset of scaling-like behavior in some reactions and kinematics has also been noted in Jefferson Lab experiments. The understanding of these issues is not yet theoretically established.

30. A.V. Radyushkin, Acta Phys. Polon. B 30, 3647 (1999) and hep-ph/0011383; A.V. Radyushkin, Phys. Lett. B 449, 81 (1999) and hep-ph/9810466; Phys. Rev. D 59, 014030 (1999) and hep-ph/9805342; I.V. Musatov, A.V. Radyushkin, Phys. Rev. D 61, 074027 (2000) and hep-ph/9905342.
31. "QCD and Rescattering in Nuclear Targets," J. Qiu, G. Sterman, hep-ph/0111002, 31 October 2001.
32. M. Luo, J. Qiu, G. Sterman, Phys. Lett. B279 (1992) 377, Phys. Rev. D49 (1994) 4493, and Phys. Rev. D50 (1994) 1951; X. Guo, J. Qiu, Phys. Rev D53 (1996) 6144, and Phys. Rev. D61 (2000) 096003; X. Guo, Phys. Rev. D58 (1998) 114033 and hep-ph/9804234.

In conclusion, the problem of factorization in moderate-energy nuclear processes has already received a significant amount of theoretical attention over the past decade. It is likely to receive continued attention for several reasons. Understanding the RHIC data will require a significant amount of effort focused on few-GeV partons in the nuclear medium, exactly the energy range of this proposed measurement. The processes of quark hadronization, quark propagation, and hadron propagation through hot nuclear systems will have to be understood in detail in order to study the properties of the system formed in relativistic heavy ion collisions. Factorization at low Q^2 in low-x processes has already been demonstrated in HERA data.

SUMMARY OF OBSERVABLES

To summarize the variables and observables discussed above, given certain assumptions concerning coherence properties of the gluon radiation, the energy loss *may* vary with energy as:

$$\frac{-dE}{dx} \propto \sqrt{E} \quad \textbf{(EQ 8)}$$

with the transverse momentum broadening as:

$$\frac{-dE}{dx} \propto \Delta < k_{\perp}^{2} > \quad \textbf{(EQ 9)}$$

and, assuming $\Delta < k_{\perp}^{2} > \propto$ L, with distance L through the medium as:

$$\frac{-dE}{dx} \propto L \quad \textbf{(EQ 10)}$$

which leads to the quadratic total energy loss.

Insight into any energy dependence of the energy loss may be gained by combining measurements from the proposed data with existing measurements from HERMES and Fermilab. It should be possible to directly measure the transverse momentum broadening as a function of the parton energy and the distance through the medium. Using Equation 6 as guidance for the size of the broadening to be expected, and assuming the intrinsic quark transverse momentum Gaussian parameter in the nucleon is 0.44 GeV (a typical value), then the additional broadening due to nuclear effects should vary from zero for the smallest nucleus to 0.120 GeV^2 for Au, a few hundred MeV effect that should be easily measurable with the momentum resolution of CLAS. This is discussed further in ’‘Resolution issues” on page 35.

Space-Time Characteristics of Hadronization: Scientific Significance and Present Status

CONFINEMENT

Quark hadronization is a fundamentally non-perturbative process that is intimately linked to confinement, a central problem in hadronic and nuclear physics[33].

SPACE-TIME PICTURE OF HADRONIZATION

Decades of work on understanding hadronization at high energies have resulted in sophisticated models that predict the outgoing particle spectrum quite well for proton and neutron targets, even down to relatively low energies. Nonetheless, there is little solid information available on the space-time development of the process. For example, the functional form of the formation length is not known from a fundamental theory; even the variables which determine it are not known with certainty, although the energy of the propagating quark ν is clearly the most important, and there may be a dependence on z as a measure of the extent of gluon emission.

A plausible physical picture of quark hadronization in DIS[34] in the space-time domain is that the quark is struck within a small interval of size ~$1/E_{quark}$ (=0.05 fm for ν=4 GeV) and the semi-dressed, knocked-out quark begins radiating gluons and rebuilding its color field as it travels; the process of regeneration of the local color field, in analogy with the QED and classical electrodynamics cases, requires a space-time interval of:

$$\tau^{hadr} \approx \frac{E_q}{\mu} R_h \qquad \textbf{(EQ 11)}$$

where τ^{hadr} is the hadronization (or formation, or regeneration) length, E_q is the quark energy (= ν), μ is a soft scale comparable to the constituent quark mass, and R_h is a measure of the interquark distances in the hadron. Taking E_q=4 GeV, μ=0.3 GeV, and R_h=0.7 fm (as suggested in [34]), one finds τ^{hadr}~9 fm. Since this is comparable to the size of atomic nuclei, this suggests one can hope to use nuclei of varying size as a ‘filter’ to analyze the formation lengths.

An experimental check on this estimate comes from the already-referenced measurement by the HERMES collaboration [1] who found a good description of their DIS data on nitrogen was obtained with the form

$$\tau_f^{\pi} = 1.4(1-z)\nu \quad fm \qquad \textbf{(EQ 12)}$$

for positive and negative pions (for protons, the coefficient was 3.5 instead of 1.4). Choosing representative values from their data of ν=15 GeV and z=0.75 yields a formation length of 5 fm, reasonably consistent with nuclear dimensions and with the previous schematic example, which had no z dependence. The form of the z dependence in Equation 12 implies considerable flexibility in the ranges of the formation length, particularly for fluctuations to smaller lengths.

33. “Key Issues in Hadronic Physics,” S. Capstick, S. Dytman, R. Holt, X. Ji, J. Negele, E. Swanson, hep-ph/0012238, 18 December 2000.

34. “Basics of Perturbative QCD,” Yu. L. Dokshitzer, V.A. Khoze, A.H. Mueller, S.I. Troyan, (book) Editions Frontieres press (1991), Chapter 1.

HADRONIZATION WITHIN NUCLEI

A physical picture of hadronization within a nucleus begins with the hard scattering on a quark within a nucleon located anywhere within the nuclear volume. When the hadronization process is initiated on a quark within a nucleus within a small space-time volume, the emerging off-shell quark has the opportunity to interact with the nuclear medium. This could be viewed as a quark-nucleon interaction or a quark-quark interaction. The cross section for this interaction is not well known (and perhaps not well defined), however, the experimental indications are that it is quite small; an early study[35] using the CERN EMC data interpreted by a formation-time model[36] derived a value for the effective quark-nucleon cross section of 2 mb. While this should perhaps not be taken too seriously, the Hermes data are also consistent with a small interaction probability of the propagating quark within the nuclear medium (the values they derived ranged from 0 to 0.75 mb), as are the Drell-Yan experiments and other analyses[37]. It essentially can be seen in the region of small absorption, > 0.95, in Figure 3. The low probability of interaction has been interpreted[38] as a suppression of gluon bremsstrahlung by a formation-zone phenomenon similar to that seen in QED; a lower bound can be obtained from the *gluon* formation length, which is $\tau_{gluon}^{form} \approx \frac{k}{k_\perp^2}$ [34].

In the case when the hadron is substantially regenerated while within the nucleus, it can then interact vigorously with the nuclear medium via the much larger (tens of mb) cross sections. This results in an attenuation of the hadron in larger nuclei relative to smaller nuclei.

In the proposed measurement, the dependence of the hadronic multiplicity ratio R_M^h on variables such as ν and z will signal the region where the hadronization is taking place primarily outside the nucleus.

FORMATION LENGTH

There are a number of model predictions for the space-time behavior of hadronization that have been developed over the past three decades. These are variously based upon such pictures as: quark ‘decay time’ estimates using a single characteristic time[36], time dilation of intrinsic sizes[39], two-time-scale parameterizations based on the Lund model[40], QCD-based models[41], and a gluon-bremsstrahlung model[42]. Predictions from these are summarized in Table 1.

35. “A study of Forward Hadron Production in Deep Inelastic Muon-Nucleus Scattering,” W.J. Womersley, Thesis, Oxford (1986).
36. A. Bialas, T. Chmaj, Phys. Lett 133B, 241 (1983).
37. N. Pavel, Nucl. Phys. A 532 (1991) 465c.
38. S. J. Brodsky, G.T. Bodwin, G.P. Lepage, Proc. Int. Conf. on Multiparticle Dynamics, Volendam, 1982, p. 841.
39. “Space-Time Structure of Hadronic Collisions and Nuclear Multiple Production,” K. Gottfried, Phys. Rev. Lett. 32, 957(1974).
40. A. Bialas, M. Gyulassy, Nucl. Phys. B291, 793(1987); T. Chmaj, Acta Phys. Pol. B18 (1987(1131.
41. S.J. Brodsky, A.H. Mueller, SLAC-PUB-4615 (1988).

As may be seen, the variety of approaches could be greatly constrained with more data

TABLE 1. Formation length formulae from various models.

Model Approach	Formula	Reference
single time-scale model	$\tau = \tau_q \frac{E_{quark}}{m_{quark}} \sim \upsilon$	[36]
time dilation of intrinsic size	$\tau = \tau_0 \frac{E_{hadron}}{m_{hadron}} = \tau_0 \frac{z\upsilon}{m_{hadron}}$	[39] (typical)
two-timescale parameterization based on the Lund model	$\tau = (1 - \ln(z)) \frac{z\nu}{\kappa c}$	[40]
QCD-based model	$\tau \approx \frac{1}{c} \frac{r_{hadron}}{k_{hadron}} E_h \sim z\nu$	[41]
gluon-bremsstrahlung model	$\tau = c_{hadron}(1-z)\nu$	[42]

that spans a wider range of kinematic variables and nuclei, especially one with enough statistics to allow multidimensional analysis. At the least, the relevant degrees of freedom can be better identified.

Hadronization - Energy Loss Connection

Although the topics of hadronization and energy loss have been discussed independently above, there are strong connections between the two, both theoretically and experimentally.

A propagating quark can always emit gluons, whether in a nuclear medium or not. Whether the quark is rebuilding its own local color field as in hadronization, or losing energy via radiative processes, both phenomena have an immediate connection to gluon radiation. Therefore, a complete separation of the two processes is conceptually impossible. This has important theoretical and experimental implications for using the nuclear medium to measure either one.

An interesting example that illustrates the issues may be taken from the earlier discussion of the HERMES data and its analysis by references [1] and [21]. In reference [1], the HERMES measurement of DIS on nitrogen with a 27 GeV positron beam was analyzed to extract information on formation lengths, based on the attenuation of hadrons

42. B. Kopeliovich, J. Nemchik, E. Predazzi, Proceedings of the Workshop on Future Physics at HERA, edited by G. Ingelmann, A. DeRoeck, R. Klanner, DESY, 1995/1996, vol. 2, 1038 and nucl-th/9607036.

as a function of z and ν. Their result for pions was given in Equation 12, $\tau_f^{\pi} = 1.4(1-z)\nu \quad fm$. Assuming this equation is correct, for z = 0.9 and ν = 8 GeV, the formation length is only about 1 fm, much smaller than the nuclear radius. In the midrange of the data, using ν = 15 GeV and z = 0.5, one finds about 10 fm, a much larger value; however, the nuclear radii of nitrogen (2.7 fm) and krypton (4.9 fm) that were used in the analysis of [21] are still comparable in size to 10 fm, and quite different from each other. Further, the part of the data that most influences the results of that analysis are at low ν and high z, where the attenuation is largest (see Figure 2 and Figure 3) and the formation length is shortest. The analysis of [1] attributed the reduction in multiplicity to hadronization effects. The analysis of [21] attributed it only to partonic energy loss, assuming *no* hadronization took place. The two analyses cannot be simultaneously correct.

It is clear that both energy loss and hadronization are contributing at some level to the Hermes data. Paradoxically, it appears to be possible with the present data to interpret attenuation of hadrons in nuclei in terms of either effect. While the analysis of [21] was far more sophisticated than that of [1], it relied on the approximation that hadronization within the nucleus was negligible. Since the present understanding of the space-time characteristics of hadronization is still at a primitive stage, the accuracy of this approximation is not known.

Obtaining more data at lower energies for a variety of nuclei should help to sort out the hadronization effects from the energy loss effects and resolve this perplexing ambiguity. In addition, combining the information from p_T broadening with that from the fragmentation functions on the same nucleus will provide valuable additional constraints that are partially independent; a more consistent picture may emerge from using both pieces of information. This will be possible in the experiment proposed here. Further, more sophisticated theoretical modeling of the hadronization part of the process will probably be necessary.

An additional exercise which may help to isolate hadronization effects is to compare pion and kaon production for a momentum of 2 GeV/c, where the formation length will be small but the K^+N and πN interactions are very different. In general, the production rate of K^+ will be reasonably high due to the high luminosity, so that additional information on the flavor dependence of hadronization and energy loss will be accessible. However, the combination of incomplete particle identification of charged kaons at high momentum, and the intrinsically smaller rate, will limit these studies to more of an exploratory mode.

3.2 Experimental Method in CLAS

SIMULATIONS

The expected data were simulated using the LEPTO version 6.5 Monte Carlo event generator for deep inelastic lepton-nucleon scattering. JETSET version 7.409 and PYTHIA version 5.721 were called by LEPTO; the parton density functions used[43] were the GRV HO set from PDFLIB version 8.01. The LEPTO event generator does not include the effect of nuclear absorption of hadronization products, but rather is fine-tuned for an accurate description of the hadronization process from the individual neutron or proton. Although this event generator has primarily been used at much higher energies, it is appropriate for use in the kinematic range which will be discussed here[44]. The calculation takes into account quark distribution functions in the protons and neutrons of the nucleus for u, d, s, c quarks and antiquarks.

The acceptance function applied to the simulated data in the following section is a parameterization based on measured data in CLAS. This parameterization depends on particle type, momentum, magnetic field setting, and lab angles. Extensive testing of such parameterizations against full GEANT simulations has demonstrated that single-particle acceptances are reproduced to better than 10%[45]. The response of CLAS to the particles emphasized below, protons and positive pions, is very well understood; the bulk of the CLAS electroproduction program has been based on measuring these over a wide range in kinematics.

Two LEPTO simulations were run and checked against the acceptance; the first had a lower Q^2 cutoff, the second had a higher Q^2 cutoff. Since LEPTO produces an integrated cross section within the user-specified cuts, its results are normalized and can be used to predict count rates. The low-cutoff simulation was used to understand the basic data topology, while the high-cutoff simulation was used for rate estimates, as will be described in more detail below. Figure 5 depicts the kinematic regions for the two simu-

TABLE 2. LEPTO simulation parameters for the low-Q^2 cutoff.

Parameter	Lower Limit	Upper Limit
x	0.15	0.69
y	0.43	0.95
Q^2 (GeV^2)	**1.5**	7.0
W (GeV)	2.0	3.1

43. Improved parton distribution functions for use at low energies have recently been developed; see “Modeling Deep Inelastic Cross Sections in the Few GeV Region,” A. Bodek, U. K. Yang, to be published in Nucl. Physics B. Proceedings Supplement, Fall 2002, and hep-ex/0203009.

44. Private communication with G. Ingelman and J. Rathsman, two of the three authors of LEPTO.

45. “Comparison of GSIM Monte Carlo and Geometric Acceptance Functions for CLAS,” M.U. Mozer, D.S. Carman, CLAS-Note 02-005, March 27, 2002.

TABLE 2. LEPTO simulation parameters for the low-Q^2 cutoff.

Parameter	Lower Limit	Upper Limit
ν (GeV)	0.01	5.4
integrated σ (nb, per nucleon)	9.6	

TABLE 3. LEPTO simulation parameters for the high-Q^2 cutoff.

Parameter	Lower Limit	Upper Limit
x	0.39	0.69
y	0.67	0.95
Q^2 (GeV^2)	**4.0**	7.0
W (GeV)	2.0	2.6
ν (GeV)	0.01	5.4
integrated σ (nb, per nucleon)	0.13	

lations. The purpose of the high Q^2 simulation was to estimate the event rate in the region which is simultaneously lowest in rate and most accessible to theoretical calculations. That kinematic region is treated as a single bin in Q^2 and ν, and can be studied with varying z. The parameters of the simulations are shown in Table 2 and Table 3.

FIGURE 5. Distribution of events in Q^2 and ν for the low-Q^2 cutoff simulation. The arrows indicate the region of the high-Q^2 cutoff simulation.

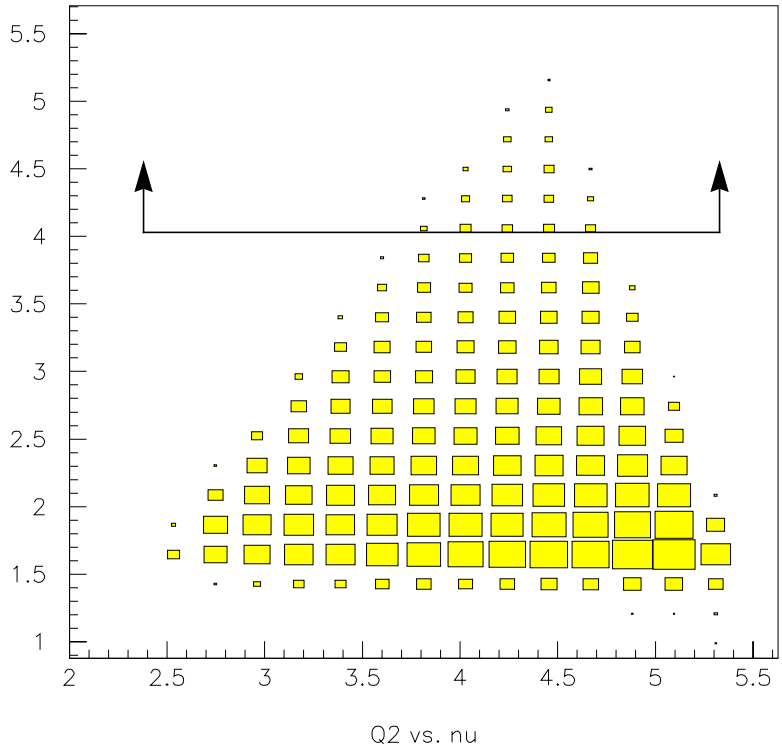

EVENT TOPOLOGY

In the following, the general features of the DIS data from the simulation will be discussed.

A plot of the event multiplicity is shown in Figure 6. All detectable particles are considered in this plot, including photons from π^0 decay and neutrons, including estimates for the photon detection threshold and the neutron detection efficiency. As may be seen, the level of complexity of the events is often high. Detecting all final state particles is prohibitive because of the finite detector acceptance, however, as may be seen, one often can detect events with multiple particles, most commonly two particles, but up to six or more with reduced acceptance. The observation of the higher-multiplicity states may provide important information on the hadronization process via the attenuation of hadronization fragments by nuclei.

FIGURE 6. Simulated event multiplicity for DIS events in CLAS, low Q^2 cut. The shaded histogram shows accepted events, and the open histogram shows thrown events. See text for more details.

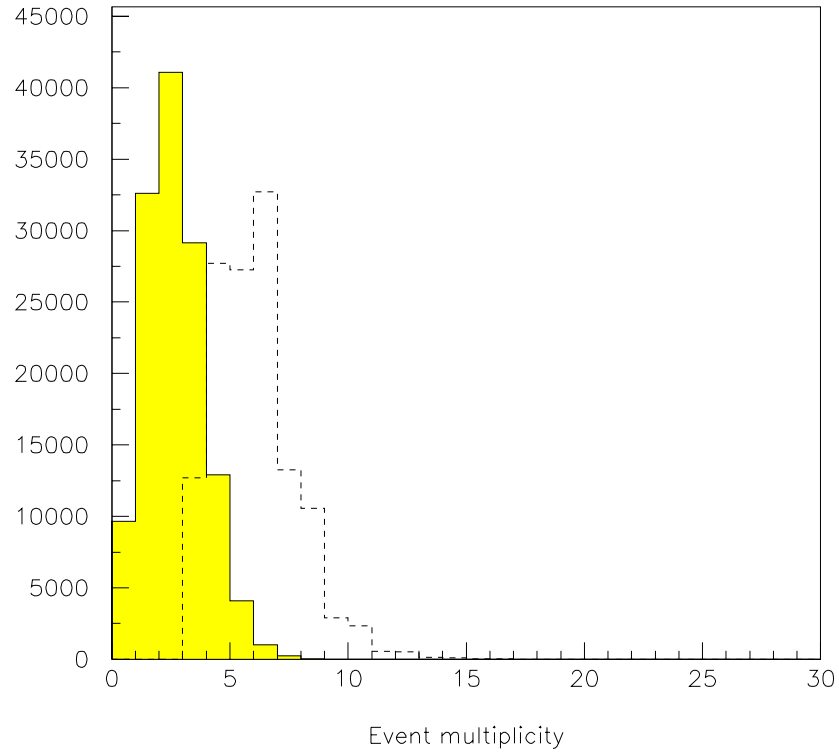

POSITIVE PION EMPHASIS

The spectrum of particle types is shown in Figure 7. In this figure, the shaded region indicates the average single-particle acceptance for that particle type, i.e., the acceptance for a two-particle final state is smaller, and it may be very crudely approximated by the product of the single particle acceptances. It may be seen that the largest acceptance is for the proton and positive pion, although there is significant acceptance for the other particle types as well. It is expected that both the theoretical calculations, and the interpretation of the data in terms of quark transport through the nuclear medium, will be most reliable for pions. Further, the interpretation is most reliable at the highest Q^2 and ν, for $z > 0.5$; for this condition on z, it is presumably not necessary to separate target fragmentation products from current fragmentation products. Finally, as will be discussed below, the particle identification coverage is most complete and unambiguous for pions relative to the other emerging particles. Therefore, *this proposal concentrates on detecting only the positive pion for most subsequent discussions and all count rate estimates*. Data from the other particle types will be analyzed to the degree permitted by statistics and particle identification (discussed briefly below).

FIGURE 7. Distribution of thrown and accepted particle types for the high-Q^2 cutoff. (Results are very similar for the low-Q^2 cutoff.) The upper panel is on a linear scale, the lower on a log scale. Neutral pions appears as decay products, primarily photons, in this plot. The number of accepted events corresponds to about 10 days of running at a luminosity of 10^{34} $cm^{-2}s^{-1}$.

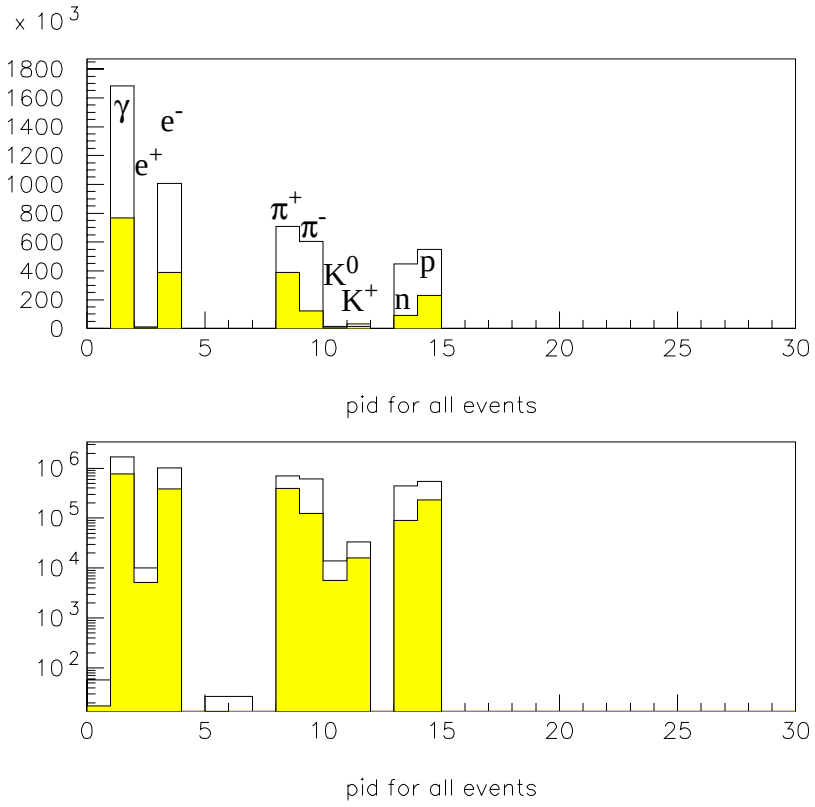

RATE OF POSITIVE PIONS

The count rate of positive pions at the highest Q^2 and ν is obtained from the simulation as follows. A plot showing the general distribution of leading pions is shown in Figure 8. The integrated cross section for the high Q^2 cutoff simulation is 0.13 nb. This simulation leads naturally to a bin in (Q^2,ν) at (4.3 GeV^2, 4.3 GeV), integrating over the other quantities subject to the cuts specified in Table 3, without integrating over z.

The CLAS luminosity limit is 10^{34} $cm^{-2}s^{-1}$ for a hydrogen target. For nuclear targets with N=Z, in principle this limit could be doubled to the extent that the background is caused by Møller electrons and the photons they produce in the shielding. However, the heavier targets produce X-rays which can cause additional background. Previous measurements in CLAS have used a reduced luminosity for running with an iron target. Since the precise experimental conditions are not yet well-characterized, for this proposal the standard limit of 10^{34} $cm^{-2}s^{-1}$ has been used.

Multiplying this luminosity by the cross section yields a rate of 1.3 Hz for DIS events in the bin of (Q^2,ν) = (4.3 GeV^2, 4.3 GeV) as specified by Table 3. The total number of

events included in this simulation was 995,000, approximately the number of events obtained in a 8.8-day run. Since the acceptance function used in this study underestimates the real acceptance function for two particles, this has been scaled by 18% to a realistic acceptance function for detection of two nearly uncorrelated particles (electron and pion, as discussed above in ''Simulations" on page 26, ultimately equivalent to a 10.4-day run. Figure 9 shows a plot indicating these statistics for leading positive pions. This plot contains 115,600 pion events, leading to a count rate estimate for leading positive pions of 0.13 Hz. Of these pions, about 60% have z>0.5, the kinematics of primary interest. The final plot of ratios of these counts, which will test the hadronization and energy loss predictions, will have statistical errors that are larger by approximately the square root of two, since the denominator of the hadronic multiplicity ratio (from deuterium) will also have similar statistical errors.

FIGURE 8. Distribution of leading positive pion counts vs. z and ν for the low-Q^2 cut simulation.

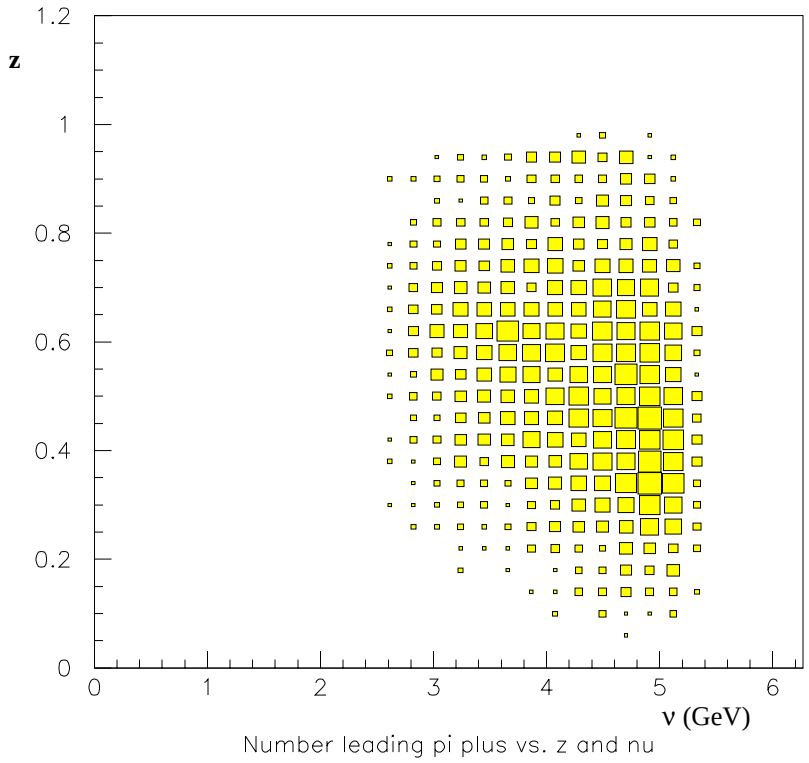

FIGURE 9. Dependence on z for a bin with Q^2=4.3 GeV^2 (from 4.0 to 5.2) and ν=4.3 GeV (from 3.8 to 4.8) for leading positive pions. These are results from the high-Q^2 cutoff simulation. The number of events shown corresponds to about 10 days of running at a luminosity of 10^{34} $cm^{-2}s^{-1}$ on one target. The structures seen are presumably an artifact of the LEPTO hadronization model.

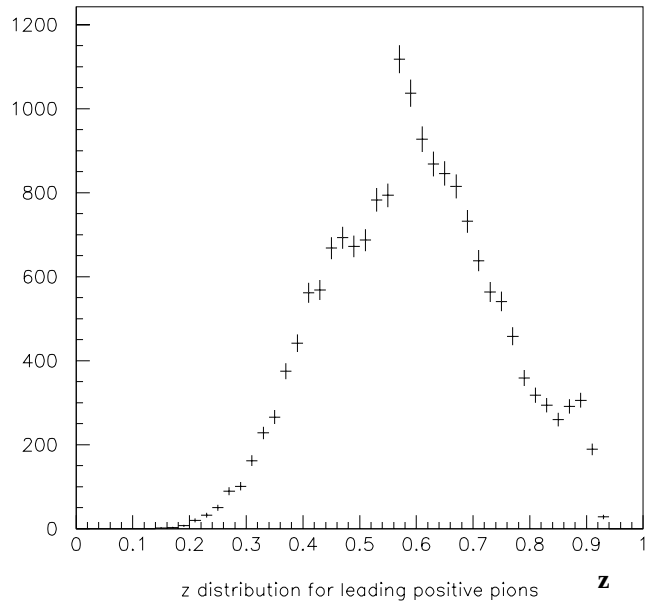

ACCEPTANCES

An approximate accounting of the averaged single particle acceptances was already shown in Figure 7. A more detailed acceptance function for the leading positive pions is shown in Figure 10. This figure displays the acceptance as a function of Q^2 and ν, and lab angle and momentum, as described in the caption. The acceptance is seen to be fairly uniform and smoothly varying.

CLAS acceptances for the other particles which might be detected (negative pions, protons, neutral pions, neutrons, charged kaons) are generally of a similar magnitude but somewhat smaller, and they differ in some details. In this discussion, the particle identification issues are considered separately, below; only the *geometrical* acceptance is emphasized here. The forward-going negative pions of lower momentum are bent into the beamline and lost, while the larger momentum, larger angle negative pions stay within the acceptance. The acceptance for non-decaying charged kaons is similar to that for non-decaying pions, and the decaying particles of each type cause some further losses; essentially those that decay outside the drift chamber volume are not lost, while many of those that decay inside the drift chamber volume (radius 3 m) are lost. The proton acceptance is similar to the positive pion acceptance. Neutrons are detected with fair efficiency from 10 degrees to 45 degrees. The neutral pion can be detected through its two-photon decay using the forward and large-angle calorimeters with a geometrical acceptance of the order of 10%. Nuclear absorption information can be derived from most of these other particles within a kinematic region that is more limited than for the positive pions.

FIGURE 10. Acceptance functions for leading positive pions from the low-Q^2 cutoff acceptance. The upper panel shows the acceptance on the vertical axis, the z values from 0.2 to 1.0 on one horizontal axis, and the ν values from 2 to 5 GeV on the other horizontal axis. On the lower panel is plotted the acceptance on the vertical axis, the lab frame momentum from 1 to 5 GeV, and the lab frame scattering angle from 0 to 50 degrees. The typical acceptance value is fairly uniform and ranges from 10-30%.

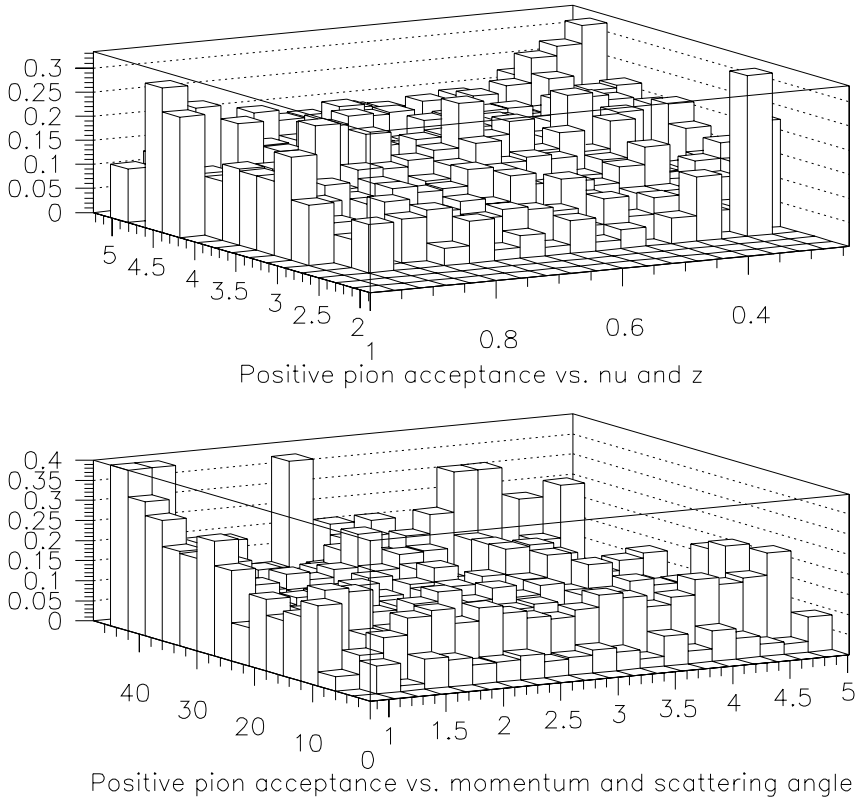

PARTICLE IDENTIFICATION

The comments below refer only to identification of the leading (highest momentum) particle. The subleading charged hadrons will generally be easier to identify because they will generally have lower momentum. The main issue here is the identification of the leading hadron.

Particle identification for the *positive pions* should be adequate over the entire range of measured kinematics. They are separated from electrons via their positive charge. Up to a momentum of 2 GeV, positive pions can be cleanly separated (3σ) from kaons via time of flight using the standard CLAS techniques used for essentially all experiments. Above 2.5 GeV, the pions will begin to emit Cerenkov light in the Cerenkov counters,

separating pions from kaons and protons. It should be noted that the Cerenkov counter has approximately a 10% inefficiency for particles curving away from the beamline such as positive pions, which necessitates an additional correction factor. In the high momentum region there will also be the potential for confusion with positrons. According to the lepto simulation, the ratio of positive pions to positrons is about two orders of magnitude (see Figure 7, log plot), therefore, this will be a small correction.

FIGURE 11. Relative rates of positive kaons, positive pions, and protons from the low Q^2 simulation vs. momentum in GeV and angle in degrees.

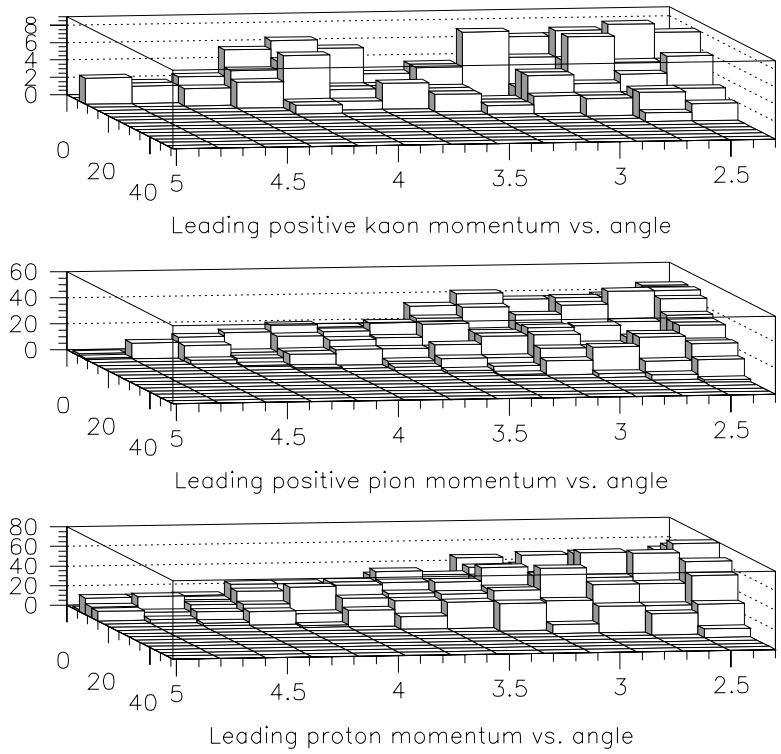

In the region from 2 - 2.5 GeV, CLAS will not be able to cleanly separate the positive pions from positive kaons. In this region, LEPTO predicts a ratio of positive pions to positive kaons of about 5:1 (see Figure 11). The time-of-flight technique will still allow some separation in this region of momentum, however, there will be some kaon contamination. Since the kaon contamination can be estimated using a model for the measured timing distributions and using the measured and modeled pion to kaon ratio, a correction to the number of pions measured can be derived, and this correction is expected to be relatively small because of the predicted 5:1 ratio. Therefore, the positive pions are adequately identified over the entire momentum range, with a few identified sources of small systematic errors.

For *negative pions*, a similar situation holds, except that they cannot be separated from the electrons by their charge. This may be somewhat easier to sort out for the highest

energy pions (high z), but in general it is a problem. The ratio of negative pions to electrons predicted by LEPTO is not favorable (see Figure 7, log plot). In the momentum range up to 2.0 GeV they can be unambiguously identified by time of flight, but above that range, more study is required to determine what information can be determined.

Charged kaons can be cleanly identified up to 2.0 GeV by time of flight. Above that momentum it will become increasingly difficult to separate them from pions until the pions emit light in the Cerenkov counter at about 2.5 GeV, but at that momentum they will begin to be confused with protons, which are more numerous.

The technique of *neutral pion* identification through direct detection of photons has been used for several CLAS analyses. Without additional kinematic constraints on the neutral pions, there will be some combinatoric backgrounds under the signal peak. It is likely that this channel can be exploited to yield useful information in this experiment, but the analysis will be more sophisticated and will depend on the details of the background. According to a recent study[46], the two photons from high-energy neutral pions can be resolved up to a momentum of 4.5 GeV. This is a very useful range of momenta for this experiment, and if the background behavior is manageable, it may yield information complementary to the positive pion data.

The prospects for identifying *protons* are fairly good for a significant range in kinematics. They can be separated from kaons by time-of-flight up to about 3.2 GeV for a 3-σ separation, and to about 4.2 GeV for a 2-σ separation, based on timing resolutions achieved for the forward plane of time of flight counters (150 ps, average) and assuming Gaussian timing distributions. At 2.5 GeV, pions begin to emit light in the Cerenkov counter, and therefore can be discriminated as discussed above. LEPTO predicts only a 3:1 ratio of protons to kaons at the highest momenta (see Figure 11). Therefore it is not clear how high in momentum above 4 GeV the proton identification can be pushed.

Although the *neutron* detection efficiency in CLAS approaches 50% for few-GeV neutrons and above, independent particle identification of neutrons is problematic. The time of flight technique is no longer useful in the momentum range of interest, and similarly, photon rejection via timing is not very efficient. It may be possible to use energy deposition patterns to accomplish a significant amount of photon discrimination, but this requires further study. Even if this is possible, there will be quite poor quality information on the neutron momentum. Therefore, it is not clear that this channel will yield useful information for this experiment.

RESOLUTION ISSUES

In general, the standard resolution of CLAS is more than adequate to accomplish the goals of this experiment, such as determining the z value for a charged pion, or the Q^2 and ν value from the electron. The one issue where the resolution needs to be discussed is in the momentum broadening measurement.

A GEANT simulation of CLAS, using realistic parameters for drift chamber resolution, shows that the predicted broadening due to the gold target is much bigger than that due to the combination of the CLAS resolution and the intrinsic momentum distributions

46. S. Stepanyan, private communication, study in preparation for the 12 GeV upgrade conceptual design report.

contained in LEPTO as shown in Figure 12. The upper plot shows the distribution from GEANT with the LEPTO event generator as input, and the lower plot shows the same distribution broadened to have the rms value of 0.39 as predicted by Equation 6 and the rms value of 0.28 shown in the upper plot. It appears to be straightforward to extract the broadening due to the nuclear targets with good accuracy. The statistics of this experiment should be adequate to study the broadening as a function of one or two kinematic variables.

As a check on the LEPTO simulation, preliminary data from the E1-6 run were analyzed to produce the same distribution. The results are shown in Figure 13. The distribution shape is rather different from the one shown in the upper panel of Figure 12, although the rms value is about the same in the two figures; both are small compared to the predicted broadening due to the gold target. It can be seen that the experimental data from the proton appear to have an even narrower distribution than predicted by LEPTO for an N=Z nucleus. Data from the very recent E6 run on deuterium at 5.7 GeV are not yet available, but will provide p_T distributions from deuterium for comparison.

FIGURE 12. GEANT simulation of the momentum distribution of positive pions in CLAS for the bin (Q^2,ν) = (4.3 GeV^2, 4.3 GeV), with and without the predicted momentum broadening due to the gold nucleus. The initial event distribution was from the high-Q^2 LEPTO simulation. The broadening is predicted to be easily measurable with the CLAS resolution. The experimental statistics should be adequate to study the broadening as a function of one or two kinematic variables.

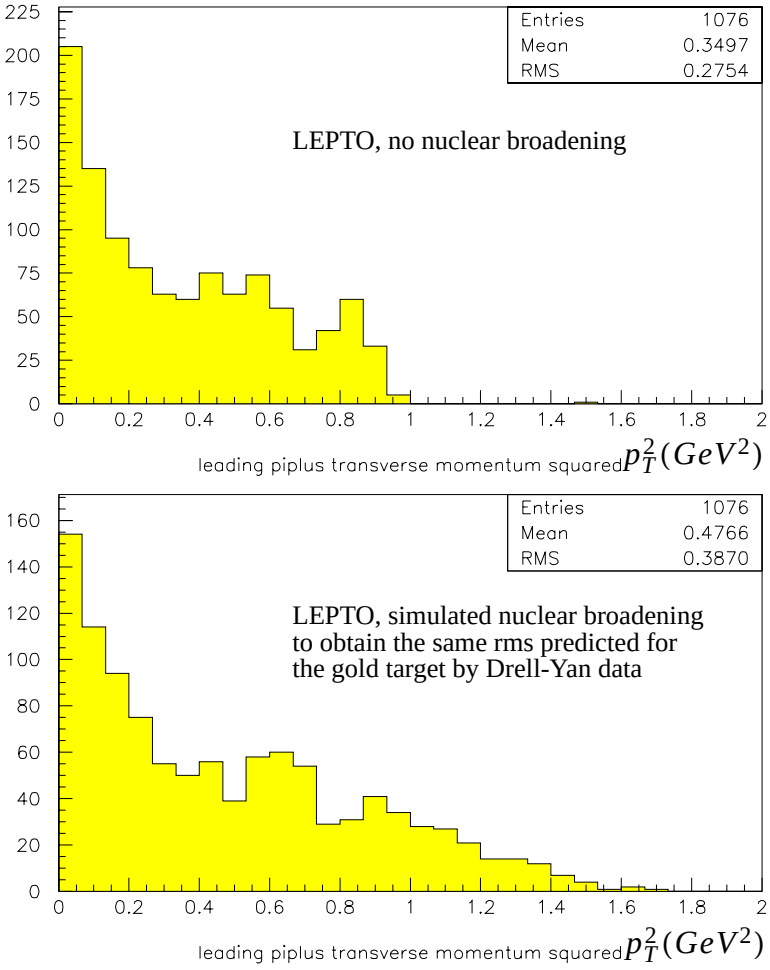

FIGURE 13. Preliminary CLAS data from the E1-6 running period. This shows the p_T^2 distribution of leading positive pions in CLAS for the same bin as in Figure 12, for a proton target and 5.7 GeV beam. By comparing the two figures, it may be seen that the shapes of the distributions are rather different, but that both of them have an rms value that is small compared to the 0.39 GeV^2 predicted by the Drell-Yan experiments. Therefore, the experimental sensitivity for measuring the momentum broadening appears to be good.

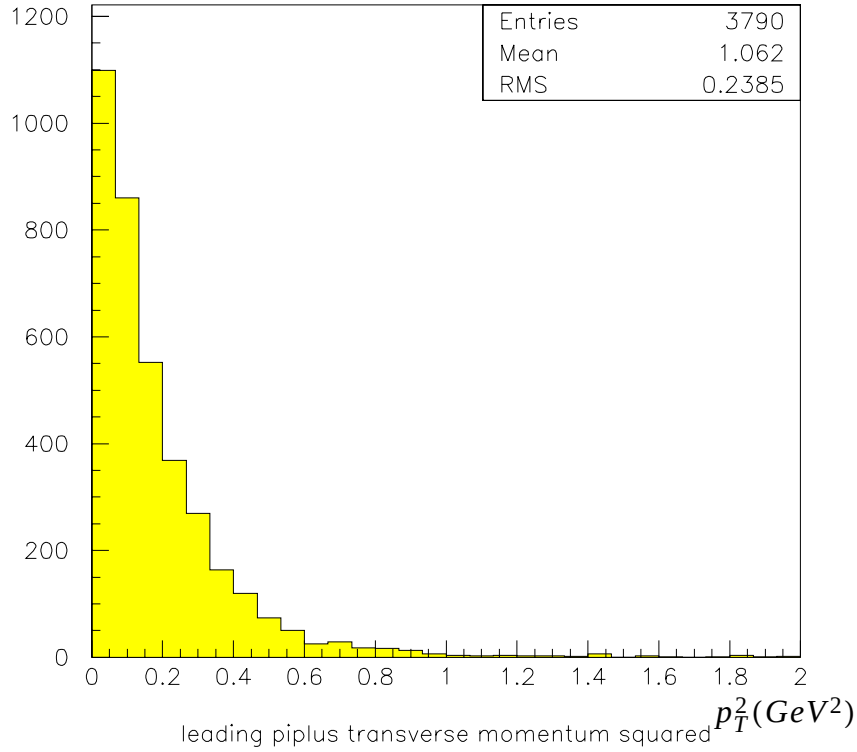

SYSTEMATIC ERRORS

The primary systematic errors that affect the positive pion measurement come from the Cerenkov counter inefficiency from particles that bend away from the beam line, from kaon contamination in the momentum range 2.0 - 2.5 GeV, from radiative corrections, and from the acceptance corrections. If fragmentation functions are to be derived, an absolute normalization error also contributes.

Since the Cerenkov counter inefficiency can be measured using specialized triggers, the pattern of inefficiency is well-known[47]. The inefficiency is due to features of the light collection that were intentionally optimized to produce very high efficiency for inbending particles (electrons in the typical magnetic field polarity) in combination with the effects of photostatistics. Therefore, these inefficiencies are fairly stable with time. The inefficiency varies somewhat, but for outbending particles it is about 10% (for inbending particles it is about 1%). We assign a systematic error of 3% to the absolute pion

47. "The CLAS Cerenkov Detector," G. Adams et al., Nucl. Inst. Meth. A465, 414 (2001).

yield for momenta above 2.5 GeV due to this effect, which will be nearly eliminated in a ratio quantity.

The effect of kaon contamination in the momentum region of 2.0-2.5 GeV is suppressed by a 6:1 pion to kaon ratio, i.e., in the limit of total confusion of the two without correction it is approximately a 17% effect. Since the time of flight method still has some rejection power in that region, and fairly reliable models such as LEPTO can predict the pion to kaon ratio, this may be a negligible effect, however, we allow a 3% error for this correction to the absolute pion yield. This will be somewhat reduced in a ratio quantity.

Guidelines for estimating the effects of radiative corrections may be taken from the HERMES paper [1]. In that paper, a systematic error of 3% or less is quoted due to radiative corrections, using a cut on y limiting it to 0.85. Their statement is that the majority of this correction cancels by taking a ratio. We therefore estimate that error at 3%, based on their experience. Those authors also quote a systematic error of 2-3% due to theoretical corrections from color transparency and soft gluon radiation. We assign an error of 3% for these effects, which are explained in more detail in the reference.

There is much experience in calculating CLAS acceptances for complicated final states. Where tests are possible, such as in elastic scattering, or for well-known cross sections, the acceptances have given correct results at the 5% level after extensive attention is paid to the simulation. Since the proposed measurement here is a ratio quantity, the acceptance correction approximately cancels. We assign a residual error of 3% to account for this effect, since the experiment does combine solid targets with extended liquid or gas targets, which will have a slightly different acceptance.

If the above-quoted systematic errors are added in quadrature, one obtains an error on the hadronic multiplicity ratio of about 6%. We adopt this as an initial estimate of the systematic errors. The systematic error on the momentum broadening measurement is likely to be smaller than the momentum resolution and is likely to be dominated by statistical effects.

FRAGMENTATION FUNCTIONS

Because of the possible effects due to the nuclear medium, it is not possible to quantitatively predict whether it will be possible to separate target fragmentation from current fragmentation. For this reason, the proposed experiments relies on high z as an indication that the particle is produced from current fragmentation. Study of the data will reveal whether further information can be obtained. If possible, it is desirable to go to lower z, to increase the sensitivity of the comparison to theoretical calculations.

The measurement of absolute fragmentation functions, e.g. in a parton model picture, entails some normalization error which will probably exceed the 6% systematic errors discussed above. A quantitative estimate is not provided in this proposal.

TARGET SELECTION AND BEAM TIME REQUEST

A summary of the targets proposed to be used is shown in Table 4. The selection is

Table 4: Targets and running days for the measurement.

Target type	Radius (fm)	Running days
^{1}H	0.8	0 (E1-6 data)
^{2}H	1.4	0 (E6 data)
^{14}N	2.7	6
^{40}Ar	3.8	8
^{84}Kr	4.9	10
^{197}Au	6.5	12
Total days		36

based on the following criteria. (1) overlap with the previous HERMES targets of nitrogen and krypton so that a consistent comparison can be made, (2) including a very heavy target (gold) to emphasize the quadratic energy loss, (3) including a range of nuclei so that any linear energy loss term can be identified, (4) assumes that the E1-6 data and the E6 data can be used for the hydrogen and deuterium data at 5.7 GeV. More beam time is allowed for the heavier nuclei in order to partially offset the anticipated loss in statistics due to nuclear absorption.

Most of the targets listed are gases at room temperature. The heaviest target will be a thin foil of gold, which will allow the flexibility to choose beam currents and foil thicknesses that are compatible with the CLAS luminosity limits. The lighter gases can be used in a standard cryotarget format as a cryogenic liquid, and the beam current will be adjusted to stay within the luminosity limits. For the heavier gas targets it will probably be more practical to run them as cooled gases, rather than cryogenic liquids, which would require the adjustment of beam currents over two orders of magnitude.

EXAMPLE RESULTS

Several plots showing one type of result from this experiment are presented in this section. The expected data is obtained by taking the statistics predicted by the simulation and the running times shown in Table 4 and scaling them using calculations of the gluon bremsstrahlung model[48] made specifically for this proposal. The calculations are only for leading pions with $z > 0.5$. The data projection is extrapolated to lower z based on the predicted dependence for $z > 0.5$ to give a schematic illustration of the appearance of the final dataset.

While the dependence on z is shown in the following plots, the proposed kinematics covers a range in Q^2, ν, p_T, z, and ϕ for several different particle types. The data can be binned so as to study the dependence on any one or even two of these variables. The z dependence is shown as a convenient illustration of the possibilities.

48. See e.g., 'Hadronization in Nuclear Environment,' B. Kopeliovich, J. Nemchik, E. Predazzi, nucl-th/9607036 for advance predictions of a gluon-bremsstrahlung model that agrees well with recent Hermes data.

FIGURE 14. Expected $R_M^{\pi^+}$ data for ν=4 GeV, Q^2=4 GeV^2. The lines are model calculations from a gluon bremsstrahlung model, see text.

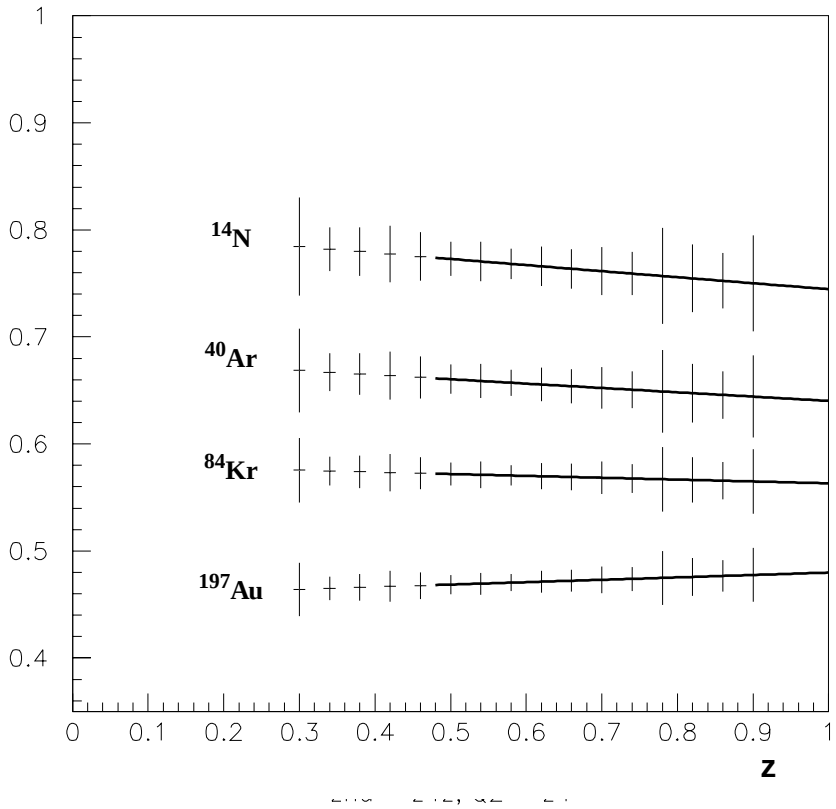

FIGURE 15. **Expected $R_M^{\pi^+}$ data for ν=5 GeV, Q^2=3 (left) and 2 (right) GeV^2. The lines are model calculations from a gluon bremsstrahlung model, see text.**

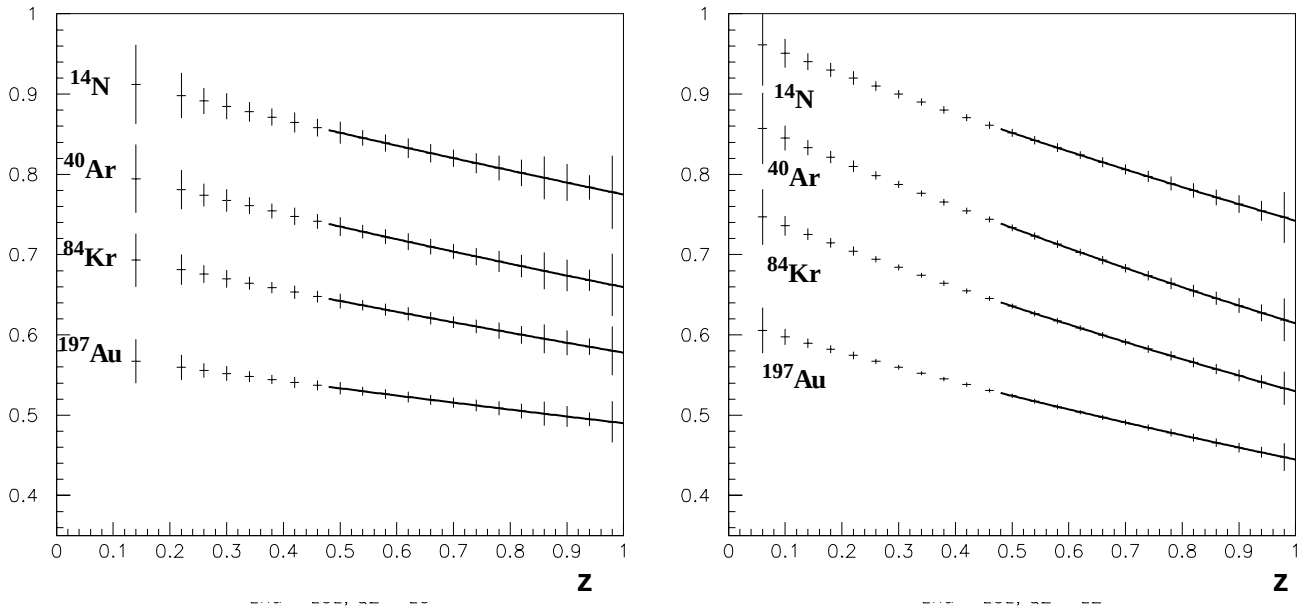

FIGURE 16. **Expected $R_M^{\pi^+}$ data for ν=4 GeV, Q^2=3 (left) and 2 (right) GeV^2. The lines are model calculations from a gluon bremsstrahlung model, see text.**

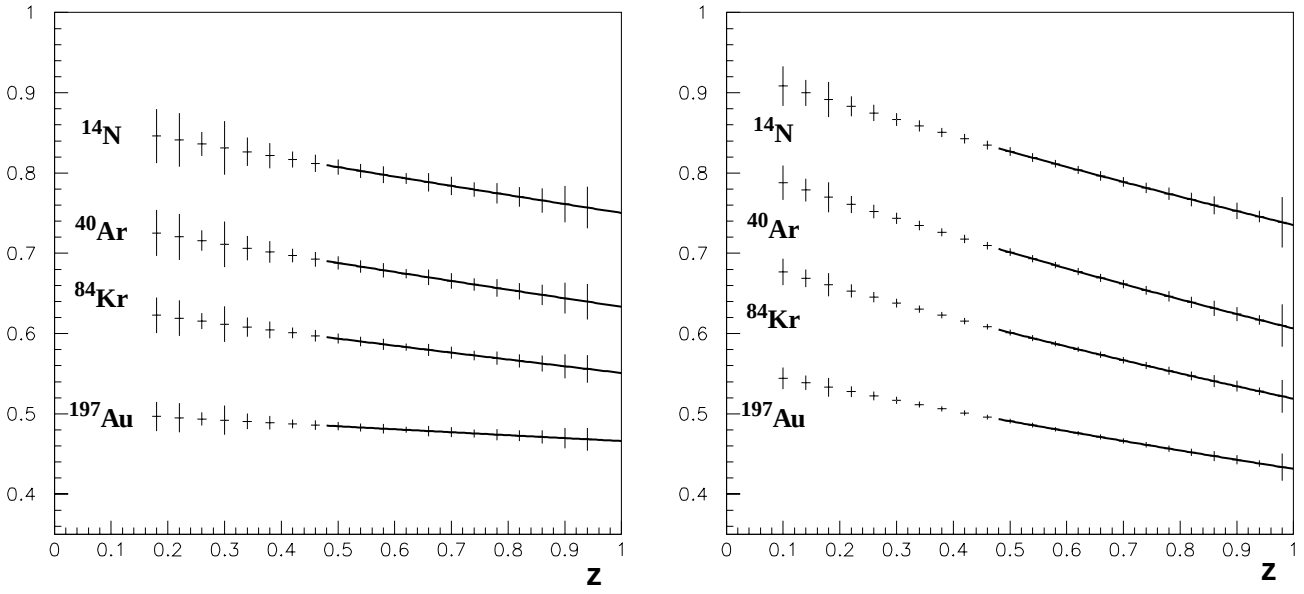

FIGURE 17. Expected $R_M^{\pi^+}$ data for ν=3 GeV, Q^2=3 (left) and 2 (right) GeV^2. The lines are model calculations from a gluon bremsstrahlung model, see text.

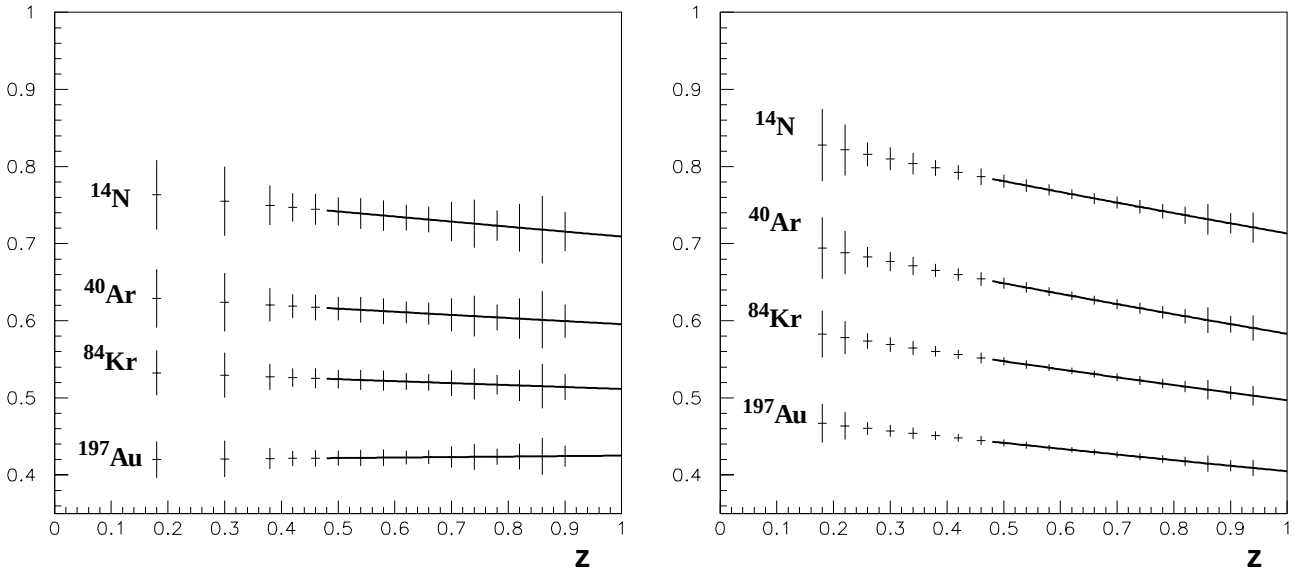

Conclusions

An outstanding opportunity exists for shedding experimental light on quark propagation through nuclei at Jefferson Lab. This is a topic of interest to several international physics communities, connecting to related studies at HERMES, RHIC, Fermilab, and the future heavy ion program at LHC. It will set the stage for a much broader study a decade later at an upgraded Jefferson Lab with an upgraded CLAS. New information on quark energy loss will improve our understanding of the radiation of gluons by quarks. Characterization of the space-time behavior of hadronization will offer new insights into the topic of quark confinement.